ANALYTICAL SOLUTION OF THE DISTRIBUTIVE THRUST FORCES DUE TO STORM SURGES IN COASTAL AREA
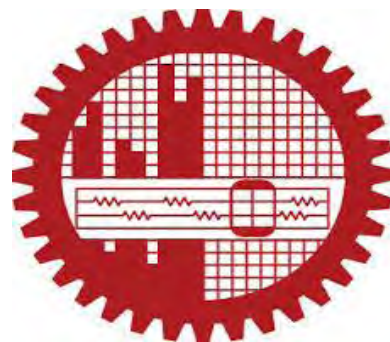
Submitted by

Marin Akter
Student No. 1014092501
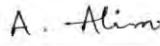Registration No. 1014092501, Session: October-2014

MASTER OF SCIENCE
IN
MATHEMATICS

Department of Mathematics
Bangladesh University of Engineering and Technology (BUET),
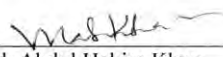Dhaka-1000
November- 2016

CERTIFICATE OF APPROVAL

The thesis entitled "**ANALYTICAL SOLUTION OF THE DISTRIBUTIVE THRUST FORCES DUE TO STORM SURGES IN COASTAL AREA**", submitted by Marin Akter, Roll No. 1014092501F, Registration No. 1014092501, Session: Octber-2014, has been accepted as satisfactory in partial fulfillment of the requirements for the degree of Master of Science in Mathematics on 22nd November, 2016.

Board of Examiners

1. _____

   Dr. Md. Abdul Alim   Chairman
   Professor   (Supervisor)
   Department of Mathematics, BUET, Dhaka

2. _____

   Head
   Department of Mathematics, BUET, Dhaka   Member
                                                                   (Ex-Officio)

3. _____

   Dr. Md. Abdul Hakim Khan
   Professor   Member
   Department of Mathematics, BUET, Dhaka

4. _____

   Dr. Md. Elias
   Professor   Member
   Department of Mathematics, BUET, Dhaka

5. _____

   Dr. Mohammad Anisul Haque   Member
   Professor   (External)
   IWFM, BUET, Dhaka
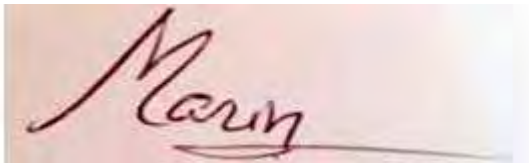
Author's Declaration

I hereby announce that the work which is being presented in this thesis entitled

"ANALYTICAL SOLUTION OF THE DISTRIBUTIVE THRUST FORCES DUE TO STORM SURGES IN COASTAL AREA"

submitted in partial fulfillment of the requirements for the degree of Master of Science, Department of Mathematics, BUET, Dhaka, is an authentic record of my own work.

The work is also original except where indicated by and attached with special reference in the context and no part of it has been submitted for any attempt to get other degrees or diplomas.

All views expressed in the dissertation are those of the authors and in no way or by no means represent those of Bangladesh University of Engineering and Technology, Dhaka. This dissertation has not been submitted to any other University for examination either in home or abroad.

(Marin Akter)
Date: 22nd November, 2016

Dedicated to,

My Parents and Teachers

Acknowledgement

Finally I express my devoted affection all of my family members and relatives specially my parents for creating a delightful atmosphere as well as excusing me from family duties in order to complete the courses, research studies and final production of the thesis work.

Author

Abstract

Most of the countries in the tropical area of the world are threatened by storm surge generated by cyclonic wind. Storm surges are generated by cyclonic winds and the atmospheric pressure drop associated with a cyclone. The major contribution comes from the winds that exert a stress on water surface which is proportional to the square of wind velocity. In addition to human lives, storm surges cause severe damages to the coastal infrastructure due to tremendous force exerted by the surge wave on these structures. To assess the damage on coastal infrastructure, an essential parameter is the resultant force exerted on these structures. To evaluate these damages, there is hardly any quantitative method available to compute this force. In this research we have developed an analytical model, named as Dynamic Force Model (DFM), by using Variational Iteration Method to compute the distributive thrust force which is generated by the cyclonic wind and moving surge. As governing equations, we have used the Saint-Venant equations which are basically 1D shallow water equations derived from the Navier-Stokes equations. During solution, steady and uniform state of flow represented by Manning's equation is used as initial condition.

The model is verified by applying the model in a hypothetical channel on which wind is blowing. The computed water velocityby analytical solution is compared with a finite difference solution and reasonable agreement is found. Wind drag coefficient is used as the calibration parameter. It is found that wind drag coefficient increases with the increase of wind speed. Flow field of DFM is validated by comparing the surge velocity computed by DFM with the surge velocity computed by a numerical model Delft3D. The coastal zone of Bangladesh is selected as the study area during model validation.

After verification, calibration and validation – the DFM is applied in the coastal zone of Bangladesh. The model computes distributive thrust force in the entire coastal zone for the following events (1) Cyclone SIDR (2) 1991 cyclone (3) Hypothetical SIDR-like cyclone (4) Impact of Sunadarban (5) Impacts of coastal afforestation (6) Impacts of coastal embankments. The results show that the model is capable to compute spatial variation of thrust forces due to cyclones of different intensities and landfall locations. The model is also capable to compute the distributive thrust force due buffering effect of Sundarban mangrove forest and artificial afforestation along the coastal belt. The model can differentiate the thrust force due to the momentum of cyclone wind only and combined impact of cyclone wind & surge wave.

Contents

Nomenclature

u_w	cyclonic wind speed
$\rho = \rho_w$	water density
C_d	Water drag coefficient
ρ_a	Air density (m/s^2)
C_w	Wind drag coefficient
h	Surge depth(m)
u	Surge velocity/water flow velocity (m/s)
A	Cross-sectional area/Area of each grid
a	Acceleration (m/s^2)
F	Thrust force (kN/m)
n	roughness of Chezy and Manning coefficient
F_p	Pressure force
z	topography
P(z)	pressure at level z
w(z)	width at level z
g	gravity
dv	small volume of a slice
dx	small length of a slice
dt	small time
θ	Slope angle
τ_b	bottom stress
τ	Reynolds stress
$u^{'}$	Turbulent fluctuation
S_f	Frictional slope
S_0	Bed slope
R_h	Hydraulic radius
w	width
B	width of each grid
F_w	wind force
L	linear operator
N	non-linear operator
g(t)	analytical function
u_n	n^{th} number iterated velocity
λ	Lagrange multiplier

τ_w wind shear stress

$\frac{\partial h}{\partial x}$ water surface slope

Subscript

n	number of iteration
b	bottom
w	wind

List of Tables

List of Figures

Chapter 1

Introduction

1.1 Background of the study

Tropical cyclones create storm surges that can strike densely populated coastal regions with devastating force (Dasgupta et al., 2009). During the past 200 years, 2.6 million people may have drowned during surge events (Nicholls. 2003) (Dashupta et al., 2009). These disasters have continued to inflict heavy losses on the people of developing countries. The most severe surge events have killed hundreds of thousands of people and inflicted extraordinary economic losses. For examples, the 1970 Bhola Cyclone generated a 9.1m storm surge in Bangladesh that killed approximately 300,000 people (Frank and Husain, 1971; Dube et al., 1997). In 2005, Hurricane Katrina inflicted $149 billion in losses (adjusted to 2013 Consumer Price Index), making it the most costly natural disaster in U.S. history (National Climate Data Center, 2014) and three times more costly than any non storm surge disaster in the U.S. Cyclone SIDR struck Bangladesh in November 2007, killing over 3,000 people, injuring over 50,000, damaging or destroying over 1.5 million homes, and affecting the livelihoods of over 7 million people (UN 2007; BDMIC 2007; IWFM 2007). Cyclone NARGIS struck Myanmar's Irrawaddy delta in May 2008, and created the worst natural disaster in the country's recorded history (Dasgupta et al., 2009). It killed over 80,000 people and affected the livelihoods of over 7 million (UN 2009) (Dasgupta et al., 2009).

The destruction due to the storm surge flooding is a serious concern along the coastal regions of the countries, for example along the coasts of Bangladesh, India and Myanmar. Bangladesh is on the receiving end of about 40% of the impact of total storm surges in the world (Murtyet al., 1992).

1

Storm surges are generated by tropical and extra-tropical storms. The low barometric pressure and wind set-up combine to produce large temporary rises in sea level which have the capacity to cause extensive flooding of coastal lowlands (Dasgupta et al., 2009). They are usually associated with strong winds and large onshore waves, exacerbating damage potential compared to a flood alone. The largest surges are produced by hurricane landfalls, but extra-tropical storms (or SIDR like cyclone) can also produce large surges.

Surges are changes in sea level (either positive or negative) resulting from variations in atmospheric pressure and associated winds. They are additional to normal tides and when added to high tides they can cause extreme water levels and flooding: flooding would be most severe when a surge coincided with spring tides. Surges are most commonly produced by the passage of atmospheric tropical or extra-tropical depressions.

The strong winds that contribute to surge events are also typically associated with large storm waves. The offshore wave height is dependent upon the wind strength and the length of time the wind has been acting upon the sea surface and these waves increase sea levels and have significant potential to cause damage and exacerbate flooding.

1.2 Rationale of the study

To assess the damage on coastal infrastructure due to cyclone wind and storm surge, an essential parameter is the resultant force exerted on these structures. In most of the cases, infrastructure damages due to storm surge are assessed as a post-disaster activity (Australian aid, 2013 and Yuvraj et al., 2015).But if people can be warned about the possible damage due to an incoming surge, these damages can be reduced significantly (Australian aid, 2013). Any reliable method to predict these damages needs an accurate computation of the resultant force on coastal infrastructure threatened by an incoming storm surge (Yuvraj et al., 2015). There is hardly any quantitative method available to compute this force. In this study, a dynamic force model is developed that analytically solves the distributive thrust force exerted on the coastal infrastructure due to storm surge. By applying this model for an incoming cyclonic surge, the forces exerted on the coastal infrastructure are computed. This force can be used to estimate the damage caused by cyclone wind and storm surge.

1.3 Objectives of the Study

The specific objectives of the present research work are:

1. To develop an analytical dynamic force model to compute the thrust force due to storm surge.

2. To apply the dynamic force model for different storm surge scenarios along Bangladesh coast.

1.4 Outline of Thesis

The remainder of the thesis paper is organized as follows. Chapter 2 reviews recent scientific works related to the development of storm surge related models. Chapter 3 describes the research strategy and methodology, while Chapter 4 describes model verification, calibration and validation. In chapter 5, model applications along Bangladesh coasts are presented. Chapter 6 summarizes and concludes the study.

Chapter2

Literature Review

2.1 Introduction

The destruction due to the storm surge flooding is a serious concern along the coastal region of Bangladesh. In addition to human lives, storm surges cause severe damages to the coastal infrastructure due to tremendous force exerted by the surge wave on these structures. Large number of storm surge models have developed to assess the damages related to this event. But none of them computes thrust force due to a cyclone generated storm surge which is an essential parameter for the damage assessment.

2.2 Coastal Zone

Coastal zone means the coastal waters and the adjacent shore lands (US Coastal zone Management Act, 1972). According to the World Bank guideline (World Bank, 1996), it is the common area where land meets the sea and incorporate the shoreline as well as the adjacent coastal water. River deltas, coastal plains, wetlands, beaches and dunes, reefs, mangrove forests, lagoons are the coastal features, ―Coastal zone‖ is referred in the Mediterranean ICZM Protocol (UNEP,2008) as the geomorphologic area either side of the seashore in which the interaction between the marine and abiotic components coexisting and interacting with human communities and relevant socio economic activities.

In Bangladesh, delineation of coastal zone is aligned with the administrative boundaries for better management perspective ((MoWR, 1999). The idea later revised considering incorporating tidal water movements, salinity intrusion, and cyclones/storm surges as the governing issues for vulnerabilities and opportunities to delineate the land area of coastal zone of Bangladesh.

The coastal zone contains many ecosystems, e.g. mangrove, marine, estuary, islands, coral and sandy beaches. The Sundarbans, the world's largest single tract of mangrove forest that has been declared a World Heritage Site, is located in the western boundary of Bangladesh coastal zone.

2.3 Vulnerabilities of the Coastal Zone due to Storm Surge

The cyclone induced disaster in the Bay of Bengal is the deadliest natural hazard in the Indian sub-continent (Pattanayak et al., 2014) because of the large coastal resources dependent livelihood. The vulnerability caused by the mortality, inundation and damage in property associated with tropical cyclones is considerably high in the coastal region because of the densely populated coastal areas, substandard infra-structures, poor socio-economic conditions and shallow bathymetry (Murty et al., 1986; Dube et al., 1997, Ali, 1999).

According to the 2001 census the total population living in the coastal zone is 35.1 million that represent 28 percent of total population of the country and there are about 6.85 million households in this region. Average population density of the coastal zone is 743 per square km. In the exposed coast the population density is 482persons per square km while it is 1012 for the interior coast (WARPO, 2004).

During the fiscal year 1999-2000 the per capita gross domestic product (GDP) for the coastal zone was US$277 which is close to the national average (US$278). Sundarban plays a significant role for providing livelihood in this region. The mangrove provides the source of earning for almost 10 million people (Islam and Haque, 2004).

2.4 Cyclone and Storm Surge

Due to heavy loss of life and property storm surge associated with severe tropical cyclone is worst coastal disaster all over the world. In Bangladesh cyclone and storm surge is a regular phenomenon. The coastal regions of Bangladesh almost is hit by cyclones in pre-monsoon (April- May) or inpost-monsoon (October-November) (Haque, 1991; Khan, 1995; Debsharma, 2009; Dasgupta, 2011).

A study by McBride(1995) stated that in every year about 80 tropical storms are formed. About 6.5% of these total storms form in the North Indian Ocean (Bay of Bengal and Arabian Sea) (Neumann, 1993). Since the frequency of cyclones in the Bay of Bengal is about 5 to 6 times the frequency in the Arabian Sea (IMD, 1979), according to Ali (1999) the Bay of Bengal share comes out to be about 5.5%. Gray (1968) and Ali (1980) stated that one tenth of worlds total cyclone generate in the Bay of Bengal. A study by Mooley and Mohile (1983) found out that one sixth of the storms formed in the Bay of Bengal hit in the coast of Bangladesh.

Main factors that are responsible for the disproportional large impact of storm surges on the coast of Bangladesh are in the following:

- The phenomenon of re-curvature of tropical cyclones in the Bay of Bengal.
- Shallow continental shelf, especially in the eastern part of Bangladesh.
- High tidal range.
- Triangular shape at the head of the Bay of Bengal.
- Lowland elevation of the coast.
- High density of population and coastal defense system.

Between 1877 and 1995 Bangladesh was hit by 154 cyclones (including 43 severe cyclonic storms, 43 cyclonic storms, 68 tropical depressions). Since 1995, five severe cyclones hit coast of Bangladesh' These are: May 1997, September 1997, May 1998, November 2007 and May 2009. On average, a severe cyclone strikes Bangladesh every three years (GoB, 2009).

Systematic studies on storm surge induced damage assessment parameters are scarce. Model studies are mainly confined to simulate surge depths and its impacts (Ali 1999, Hoque 1994, Khalil, 1992).

2.5 Factors Governing the Storm Surge

Storm surges are mainly caused by the effects of wind setup due to strong onshore winds over the sea surface and the inverted barometer effect associated with pressure drops in

low-pressure systems. To comprehend the process of cyclone induced storm surge, climatology requires to examine the parameters that develops and shapes the cyclone (Needham and Keim, 2011). Such as sea surface temperature exceeding 26 degrees C (Ali, 1996; Holland, 1997; Gray, 1998), and proximity to the Inter Tropical Convergence Zone (ITCZ), or it regional manifestation, like the South Pacific Convergence Zone (SPCZ) (De Scally 2008). To ensure sufficient atmospheric lift that develops the cyclone (Ali, 1996; Dube et al., 1997; De Scally, 2008) proximity to this global band of low pressure is required.

There are several factors that affect storm surge height and inland penetration, such as coastal topography, offshore coastal shelf, storm intensity, angle of approach, storm speed and direction (Needham and Keim, 2011). While the maximum sustained wind speed at landfall & offshore, cyclone size, forward speed determines the intensity of the storm surge - the angle of approach to the coastline, bathymetry of coastal waters, coastline shape and the presence of barriers or obstructions to surge waters plays a significant role in coastal inundation.

Harris (1963) stated that the wind stress is the predominant factor that forces the storm surge and generates the catastrophic waves. Ali (1996) provided a quantitative relationship between wind speed and water heights. According to his study, as wind stress exerts a force on water that increases exponentially as wind speeds increase. Although some scientists argue that the influence of wind speed is overestimated, Kurian et al (2009) found that wind stress accounts for 80-90% of the general surge. Study by Needham (2011) noted that pre-landfall wind speeds likely influence the maximum storm surge heights to a greater extent than wind speeds at landfall, especially for hurricanes that rapidly strengthen or weaken as they approach the coast.

2.6 Modeling of Storm Surge
Storm surge model is applied to assess the damage or to address the impacts and extent of the disaster for timely detection and emergency management. Predicting the possible tracks, landfall and intensity of the cyclone assists in preparation of proper disaster management while modeling the coastal flooding due to storm surge supports in decision

making processes. Application of mathematical model can significantly improve the cyclone forecasting in respect of generation of cyclone, tracking of movement, the corresponding storm surge and the area and depth of inundation (Haque, 1992).

So far a considerable number of modeling works including model development and application have been done for the Bay of Bengal region. Number of parametric, hydrodynamic and analytical models have been developed for storm surge generation and propagation for the coast. Numerical models by Daas (1972, 1974), Jarrel (1982), Qayyum (1983), Johns and Ali (1983), Sinha (1985), Khandaker (1987), Abrol (1987), Dube (1994), Rao (1997), Henry (1997)and Murty &Flather (1994) are the notable storm surge modeling works done in the past century. Study by Madsen and Jakobsen (2004), IWM (2005,2009), Dasgupta (2009,2011), Debsharma(2007,2009, 2014), Karim (2008), Lewis (2012) and Sakib et al. (2015) are the notable modeling work done in recent time to assess the damages along the coast.

There are different models and modeling approaches available to model storm surges. Some model looked at accurate prediction of the cyclone track and intensity while other aimed to develop models to model the physical processes of storm surge and wave generation. Techniques developed by Reid and Bodine (1968), Sielecki and Wurtele (1970) and Flather &Heaps (1975) were able to simulate generation and propagation of cyclone with the coastal features.

Numerical models are developed by scientists from IIT (Indian Institute of Technology). Most of the models are ocean wave and storm surge models. These models perform successfully to predict the cyclone associated with ocean tide and peak surge height. Das (1972) is the pioneer in the development of numerical surge model in this region. Das (1972), Sinha (1984, 1997) and Dube (1983, 1985, 1986, 1989, 1991, 1997) have developed several nonlinear models to generate the storm surge scenario in the coast and compute the accurate information on the height and location of peak surge. To predict temporal and spatial sea level variations in response to meteorological disturbances, JMA's storm surge model utilizes two-dimensional shallow water equations consisting of vertically integrated momentum equations in two horizontal directions (Higaki et al., 2010).

None of the studies mentioned above consider thrust force as a storm surge parameter. As mentioned above, thrust force is an essential parameter to assess damage to the coastal infrastructure. In present study, 1D shallow water equations are analytically solved to compute the thrust force generated from the momentum of wind and water mass of surge. Wind velocity and surge depths are computed by applying Delft3D numerical model (Sakib et al., 2015).

2.7 Analytical Solution Methods of Partial Differential Equations

A wide variety of problems in mechanics, science and engineering are related with partial differential equations and they are non-linear. Nonlinearity exists everywhere, and nature is nonlinear in general. There are many techniques, such as perturbation methods, to solve nonlinear partial differential equations (PDEs). A technique known as the method of separation of variables is perhaps one of the oldest systematic methods for solving partial differential equations including the wave equation. The wave equation and its methods of solution attracted the attention of many famous mathematicians including Leonhard Euler (1707–1783), James Bernoulli (1667–1748), Daniel Bernoulli (1700–1782), J.L. Lagrange (1736–1813), and Jacques Hadamard (1865–1963). They discovered solutions in several different forms of partial differential equations. A well-known analytical method is Decomposition Method which is established by Adomain. Special attention should be paid to Adomian's decomposition method (Adomain, 1983,1988) and Liao's homotopy analysis method (Liao, 1997).With these methods, most PDEs can be successfully approximately solved without linerization or weak linerization or small perturbations. However, the approximation obtained by Adomian's method could not always satisfy all its boundary conditions, leading to error near boundaries. A successful approximation of solution for partial differential equations is established with no boundary problems by Ji-Huan He which is known as Variational Iteration Method (VIM)(He, 1997, 1998, 1999). In this study, Variational Iteration Method is used to solve the governing equations having no boundary problems. Governing equations used in this study are the Saint-Venant equations or 1D shallow water equations which are characteristically non-linear partial differential equations.

Chapter 3

Model Development

3.1 Introduction

Navier-Stokes equations are one of the major equations in Fluid Dynamics which describe ocean and river conditions. 1D Shallow water equations i.e. Saint-Venant equations derived from Navier-Stokes equation explain of water height, elevation, water level and water velocity of ocean and river. Cyclone generated storm surge are also explained by the Saint-Venant equations which are discussed in this chapter.

3.2 Governing Equations

In Fluid Dynamics, the Saint-Venant Equations (Raisinghania et al., 2003) were formulated in the 19th century by two mathematicians, Adhémar Jean Claude Barré de Saint Venant and Bousinnesque (Raisinghania, 2003). Saint-Venant equations are derived from Navier-Stokes Equations (Vreukdenhil, 1994) for shallow water flow conditions (Kubatko, 2005).The Navier-Stokes Equations are a general model which can be used to model water flows (Bessona et al., 2007, Bulatov et al., 2013). A general flood wave for 1-D situation (Bessona et al., 2007, Bulatov et al., 2013) can be described by the Saint-Venant equations.

Assumptions of St. Venant Equations that are used in this study are:

- Flow is one-dimensional.
- Flow is unsteady and non-uniform.
- Hydrostatic pressure prevails and vertical accelerations are negligible.
- Streamline curvature is small.
- Bottom slope of the channel is small.
- Manning's and Chezy's equation are used to describe resistance effects.
- The fluid is incompressible.
- The gravity force is the only one taken into account. So the influence of the Coriolis force is neglected.

- The steady uniform state of flow expressed by using Chezy and Mannings flow equation are assumed as the initial condition.

These assumptions do not affect the basic governing equations.

In this study, the shallow water equations, also known as the Saint Venant equations, for a one- dimensional plane flow (Napiorkowski et al., 2010; Moramarco et al., 1999 and Yen et al., 2004) are used to compute the thrust forces analytically.

3.2.1 Conservation of mass

In any control volume consisting of the fluid (water) under consideration, the net change of mass in the control volume due to inflow and outflow is equal to the net rate of change of mass in the control volume.

Therefore, for continuity equation,

$$\frac{\partial h}{\partial t} + \frac{\partial}{\partial x}(hu) = 0 \qquad (3.1)$$

Where h is the water depth and u is water flow velocity.

3.2.2 Conservation of momentum

This law states that the rate of change of momentum in the control volume is equal to the net forces acting on the control volume

We write that the time rate of change of momentum inside our slice is the momentum flux entering upstream, minus the momentum flux exiting downstream, plus the sum of accelerating forces (acting in the direction of the flow), and minus the sum of the decelerating forces (acting against the flow).

$$\frac{d}{dt}[\text{Momentum inside the slice}]$$

$$= \text{Momentum flux entering at } x - \text{Momentum flux exiting at } (x + dx)$$
$$+ \text{ Pressure force in the rear} - \text{Pressure force ahead}$$
$$+ \text{Downslope gravitaional force} - \text{Frictional force along the bottom}$$

$$(3.2)$$

The momentum is the mass times the velocity, i.e. $(\rho dv)u = \rho A u dx$, whereas the momentum flux is the mass flux times the velocity, i.e. $(\rho A u)u = \rho A u^2$. The pressure force F_p action at each end of the slice is obtained from the integration of the depth-dependent pressure over the cross section.

11

Pressure force $= F_p = \iint p \, dA = \int_0^h p(z)w(z)dz$ (3.3)

in which p(z) and w(z) are, respectively, the pressure and channel width at level z, with z varying from zero at the bottom-most point to h at the surface. Under the assumption of a hydrostatic balance, the pressure increases linearly with depth according to

$p(z) = \rho g(h - z)$ (3.4)

discounting the atmospheric pressure which acts all around and has no net effect on the flow. The pressure force is thus equal to:

$F_p = \int_0^h \rho g(h - z)w(z)dz$ (3.5)

and is a function of how filled the channel is. In other words, it is a function of depth h. Taking the h derivative (which will be needed later), we have:

$$\frac{dF_p}{dh} = [\rho g(z - h)w(z)]_{z=h} + \int_0^h \rho g w(z)dz$$

$= \rho g \int_0^h w(z)dz = \rho g A$ (3.6)

The gravitational force is the weight of the water slice projected along the x–direction, which is mg $(= \rho v)$ times the sine of the slope angle θ,

Gravitational force $= [(\rho dv)g]sin\theta = \rho A g S_0 dx$ (3.7)

The frictional force is the bottom stress τ_b multiplied by the wetted surface area:

Frictional force $= \tau_b p dx$ (3.8)

the bottom stress is proportional to the square of the velocity. Invoking a drag coefficient C_D, we write:

Bottom stress $= \tau_b = C_D \rho u^2$ (3.9)

which resembles a Reynolds stress $(\tau = -\rho u' w')$, with the turbulent fluctuations u' and w' each proportional to the average velocity u. The frictional force exerted on the slice of water is then:

Frictional force $= \tau_b p dx = C_D \rho u^2 p dx$ (3.10)

We now gather the momentum budget as

$$\frac{[\rho A u dx|_{at\ (t+dt)} - \rho A u dx|_{at\ t}]}{dt}$$
$$= \rho A u^2|_{at\ x} - \rho A u^2|_{at\ x+dx} + F_p|_{at\ x} - F_p|_{at\ x+dx}$$
$$+ \rho g A S_0 dx - C_D \rho u^2 p dx$$

(3.11)

In differential form,

$$\frac{\partial}{\partial t}(\rho A u) + \frac{\partial}{\partial x}(\rho A u^2) = -\frac{\partial F_p}{\partial x} + \rho g A S_0 - c_d \boldsymbol{\rho} p u^2$$ (3.12)

The gradient of the pressure force becomes

$$\frac{\partial F_p}{\partial x} = \frac{d F_p}{dh}\frac{\partial h}{\partial x} = \rho g A \frac{\partial h}{\partial x}$$ (3.13)

Which simplifies into

$$\frac{\partial u}{\partial t} + u\frac{\partial u}{\partial x} = -g\frac{\partial h}{\partial x} + g S_0 - c_D \frac{u^2}{R_h}$$ (3.14)

In this equation the ratio of the cross-sectional area A over the wetted perimeter P, which has the dimension of a length, is defined as

$$R_h = \frac{A}{P}$$ (3.15)

This is called hydraulic radius. Because we consider wide water body, which is much wider than they are deep, the wetted perimeter is generally not much more than the width $(P \approx W)$, and so the hydraulic radius is approximately

$$R_h = \frac{A}{W}$$ (3.16)

So the momentum equation reduces to

$$\frac{\partial u}{\partial t} + u\frac{\partial u}{\partial x} = -g\frac{\partial h}{\partial x} + g S_0 - c_D \frac{u^2}{R_h}$$ (3.17)

If we include the cyclonic wind term with the momentum equation and considering $\boldsymbol{\rho} = \boldsymbol{\rho}_w$=water flow velocity and $\boldsymbol{\rho}_a$=air density (3.17) becomes

$$\frac{\partial u}{\partial t} + u\frac{\partial u}{\partial x} = -g\frac{\partial h}{\partial x} + g S_0 - c_D \frac{u^2}{R_h} + \frac{\rho_a}{\rho_w R_h} C_w u_w^2$$ (3.18)

Where we have expressed wind shear stress as $\tau_w = \rho_a C_w u_w{}^2$ i.e. wind force $F_w = \tau_w B dx$, thus $F_w = \rho_a C_w u_w{}^2 B dx$; C_w is wind drag coefficient, B is width of water and ρ_a is the density of air.

Equations (3.17) and (3.18) are called the Saint-Venant equation i.e. 1D shallow water equation for open channel flow.

In present study, all these equations are solved analytically to compute spatial variation of forces exerted by the wind and water mass.

3.3 Variational Iteration Method (VIM)

In 1978, Inokuti et al. (Inokuti et al., 1978) proposed a general Lagrange multiplier method to solve non-linear problems, which was first proposed to solve problems in quantum mechanics (Inokuti et al., 1978and the references cited therein). The main feature of the method is as follows: the solution of a mathematical problem with linearization assumption is used as initial approximation or trial-function, then a more highly precise approximation at some special point can be obtained. Considering the following general non-linear system

$$Lu(t) + Nu(t) = g(t) \qquad (3.19)$$

where L is a linear operator, N is a non-linear operator and g(t) is a known analytical function.

Ji-Huan He modified the above method into an iteration method (He, 1997; Finlayson et al., 1972; He, 1998 and He, 1999) in the following way:

$$u_{n+1} = u_n + \int_0^t \lambda [Lu_n(\xi) + N\overline{u_n}(\xi) - g(\xi)]d\xi \qquad (3.20)$$

where λ is a general Lagrange multiplier (Inokuti et al., 1978), which can be identified optimally via the variational theory (Inokuti et al., 1978; He, 1999; Nayfeh et al., 1985 and Finlayson et al., 1972), the subscript n denotes the nth approximation, and u_n is considered as a restricted variation (Finlayson et al., 1972), i.e. $\delta\overline{u_n} = 0$

The method is shown to solve effectively, easily, and accurately a large class of non-linear problems with approximations converging rapidly to accurate solutions.

.

In 1997, the Variational Iteration Method (VIM) was proposed by He (He, 1997). This method is now widely used by many researchers to solve linear and nonlinear partial differential equations. The method introduces a reliable and efficient process for a wide variety of scientific and engineering applications, linear or nonlinear, homogeneous or non-homogeneous, equations and systems of equations as well. It was shown by many authors (He, 1997,1998, 1999; Abdouand Soliman, 2005) that this method is more powerful than existing techniques such as the Adomian method (Adomian 1988; Cherruault, 1989 and Hagedorn , 1981) perturbation method, etc. The method gives rapidly convergent successive approximations of the exact solution if such a solution exists; otherwise a few approximations can be used for numerical purposes. The existing numerical techniques suffer from the restrictive assumptions that are used to handle nonlinear terms. The VIM has no specific requirements, such as linearization,small parameters, Adomian polynomials, etc. for nonlinear operators. Another important advantage is that the VIM method is capable of greatly reducing the size of calculation while still maintaining high accuracy of the numerical solution. Moreover, the power of the method gives it a wider applicability in handling a large number of analytical and numerical applications.

3.4 Solution of the governing equation:

Equations (3.17) and (3.18) which are known as Saint Venant equations can be re-written as

$$\frac{\partial u}{\partial t} + u\frac{\partial u}{\partial x} + g\frac{\partial h}{\partial x} - gs_0 + C_d\frac{u^2}{R_h} = 0 \qquad (3.21)$$

and

$$\frac{\partial u}{\partial t} + u\frac{\partial u}{\partial x} + g\frac{\partial h}{\partial x} - gs_0 + C_d\frac{u^2}{R_h} - \frac{\rho_a}{\rho_w R_h}C_w{u_w}^2 = 0 \qquad (3.22)$$

Where ρ_a is air density, ρ_w is water density, u_w is cyclonic wind speed and u is water velocity.

We express the steady uniform state of flow by the Chezy and the Mannings flow equation as an initial condition for the equations (3.21) and (3.22), which means

$$u_0(x, 0) = \frac{1}{n} R_h{}^{2/3} S_0{}^{1/2} \tag{3.23}$$

where n is roughness for Chezy and Manning coefficient and R_h is hydraulic radius for open flow.

The correction functional for the equation (3.22) is

$$u_{n+1} = u_n + \int_0^t \lambda(\xi) \left[\frac{\partial u_n}{\partial \xi} + u \frac{\partial u_n}{\partial x} + g \frac{\partial h}{\partial x} - g s_0 + C_d \frac{u_n{}^2}{R_h} - \right.$$

$$\left. \frac{\rho_a}{\rho_w R_h} C_w u_w{}^2 \right] d\xi$$

$$\tag{3.24}$$

The stationary condition is given by

$$\lambda'(\xi) = 0$$

$$1 + \lambda(\xi)|_{\xi=t} = 0 \tag{3.25}$$

so that $\lambda = -1$ and substituting the value of the Lagrange multiplier into the functional (3.24)gives the iteration formula

$$u_{n+1} = u_n - \int_0^t \left[\frac{\partial u_n}{\partial \xi} + u \frac{\partial u_n}{\partial x} + g \frac{\partial h}{\partial x} - g s_0 + C_d \frac{u_n{}^2}{R_h} - \right.$$

$$\rho a \rho w R h C w u w 2 d\xi$$

$$\tag{3.26}$$

The zeroth approximations $u_0(x, 0) = \frac{1}{n} R_h{}^{2/3} S_0{}^{1/2}$ are selected by using the given initial conditions. Following are the successive approximations:

$$u_0(x, 0) = \frac{1}{n} R_h{}^{2/3} S_0{}^{1/2} \tag{3.27}$$

$$u_1 = u_0 - \int_0^t \left[\frac{\partial u_0}{\partial \xi} + u \frac{\partial u_0}{\partial x} + g \frac{\partial h}{\partial x} - g s_0 + C_d \frac{u_0{}^2}{R_h} - \frac{\rho_a}{\rho_w R_h} C_w u_w{}^2 \right] d\xi \tag{3.28}$$

$$u_1 = \frac{1}{n} R_h{}^{2/3} S_0{}^{1/2}$$

$$- \int_0^t \left[\frac{\partial}{\partial \xi} \left(\frac{1}{n} R_h{}^{2/3} S_0{}^{1/2} \right) + \frac{1}{n} R_h{}^{2/3} S_0{}^{1/2} * \frac{\partial}{\partial x} \left(\frac{1}{n} R_h{}^{2/3} S_0{}^{1/2} \right) \right.$$

$$\left. + g \frac{\partial h}{\partial x} - g s_0 + C_d \frac{1}{R_h} \left(\frac{1}{n} R_h{}^{2/3} S_0{}^{1/2} \right)^2 - \frac{\rho_a}{\rho_w R_h} C_w u_w{}^2 \right] d\xi$$

(3.29)

$$u_1 = \frac{1}{n} R_h{}^{2/3} S_0{}^{1/2}$$

$$-\int_0^t \left[g\frac{\partial h}{\partial x} - gs_0 + C_d \frac{1}{R_h}\left(\frac{1}{n} R_h{}^{2/3} S_0{}^{1/2}\right)^2 \right.$$

$$\left. -\frac{\rho_a}{\rho_w R_h}\ C_w u_w{}^2 \right] d\xi$$

(3.30)

as $\frac{\partial}{\partial x}\left(\frac{1}{n} R_h{}^{2/3} S_0{}^{1/2}\right) = \frac{\partial}{\partial \xi}\left(\frac{1}{n} R_h{}^{2/3} S_0{}^{1/2}\right) = 0$ is the steady and uniform condition.

$$u_2 = u_1 - \int_0^t \left[\frac{\partial u_1}{\partial \xi} + u\frac{\partial u_1}{\partial x} + g\frac{\partial h}{\partial x} - gs_0 + C_d \frac{u_1{}^2}{R_h} - \frac{\rho_a}{\rho_w R_h} C_w u_w{}^2 \right] d\xi \quad (3.31)$$

Using Equation (3.30) we get the 2nd iterated formula as:

$$u_2 =$$

$$\frac{1}{n} R_h{}^{2/3} S_0{}^{1/2} - \int_0^t \left[g\frac{\partial h}{\partial x} - gs_0 + C_d \frac{1}{R_h}\left(\frac{1}{n} R_h{}^{2/3} S_0{}^{1/2}\right)^2 - \frac{\rho_a}{\rho_w R_h} C_w u_w{}^2 \right] d\xi -$$

$$\int_0^t \left[\frac{\partial}{\partial \xi}\left(\frac{1}{n} R_h{}^{2/3} S_0{}^{1/2} - \int_0^t \left[g\frac{\partial h}{\partial x} - gs_0 + C_d \frac{1}{R_h}\left(\frac{1}{n} R_h{}^{2/3} S_0{}^{1/2}\right)^2 - \right. \right. \right.$$

$$\left. \left. \frac{\rho_a}{\rho_w R_h} C_w u_w{}^2 \right] d\xi \right) +$$

$$\left(\frac{1}{n} R_h{}^{2/3} S_0{}^{1/2} - \right.$$

$$\int_0^t \left[g\frac{\partial h}{\partial x} - gs_0 + C_d \frac{1}{R_h}\left(\frac{1}{n} R_h{}^{2/3} S_0{}^{1/2}\right)^2 - \right.$$

$$\left. \frac{\rho_a}{\rho_w R_h} C_w u_w{}^2 \right] d\xi \right) \frac{\partial}{\partial x}\left(\frac{1}{n} R_h{}^{2/3} S_0{}^{1/2} - \right.$$

$$\int_0^t \left[g\frac{\partial h}{\partial x} - gs_0 + C_d \frac{1}{R_h}\left(\frac{1}{n} R_h{}^{2/3} S_0{}^{1/2}\right)^2 - \frac{\rho_a}{\rho_w R_h} C_w u_w{}^2 \right] d\xi \right) + g\frac{\partial h}{\partial x} - gs_0 +$$

$$C_d \frac{1}{R_h}\left(\frac{1}{n} R_h{}^{2/3} S_0{}^{1/2} - \int_0^t \left[g\frac{\partial h}{\partial x} - gs_0 + C_d \frac{1}{R_h}\left(\frac{1}{n} R_h{}^{2/3} S_0{}^{1/2}\right)^2 - \right. \right.$$

$$\left. \left. \frac{\rho_a}{\rho_w R_h} C_w u_w{}^2 \right] d\xi \right)^2 - \frac{\rho_a}{\rho_w R_h} C_w u_w{}^2 \right] d\xi$$

$$(3.32)$$

Definite integral

Given a function f(x) that is continuous on the interval [a,b] we divide the interval into n subintervals of equal width Δx , and from each interval choose a point, x_i. Then the definite integral of f(x) from a to b is

$$\int_a^b f(x)dx = \lim_{n\to\infty}\sum_{i=1}^n f(x_i)\Delta x$$

Using definite integral, we have

$$\int_0^t g\frac{\partial h}{\partial x}d\xi \approx \sum_{\xi=0}^t g\frac{\partial h}{\partial x}\Delta\xi \text{ and } \int_0^t u_w\,d\xi \approx \sum_{\xi=0}^t u_w\Delta\xi \qquad (3.33)$$

(3.32) simplifies that

$$u_2 \approx \frac{1}{n}R_h{}^{2/3}S_0{}^{1/2} - \frac{1}{n}R_h{}^{2/3}S_0{}^{1/2}\left(\sum_{\xi=0}^{t}g\frac{\partial^2 h}{\partial x^2}\Delta\xi^2 - \frac{2\rho_a C_w}{\rho_w R_h}\sum_{\xi=0}^{t}u_w\frac{\partial u_w}{\partial x}\Delta\xi^2\right)$$

$$+\left(\sum_{\xi=0}^{t}g\frac{\partial h}{\partial x}\Delta\xi^2 - gS_0t^2 + \frac{C_d}{n^2}R_h{}^{1/3}S_0t^2\right.$$

$$\left.-\frac{C_w\rho_a}{\rho_w R_h}\sum_{\xi=0}^{t}u_w{}^2\Delta\xi^2\right)\left(\sum_{\xi=0}^{t}g\frac{\partial^2 h}{\partial x^2}\Delta\xi - \frac{2\rho_a C_w}{\rho_w R_h}\sum_{\xi=0}^{t}u_w\frac{\partial u_w}{\partial x}\Delta\xi\right)$$

$$-\left(\sum_{\xi=0}^{t}g\frac{\partial h}{\partial x}\Delta\xi - gS_0t + \frac{C_d}{n^2}R_h{}^{1/3}S_0t - \frac{C_w\rho_a}{\rho_w R_h}\sum_{\xi=0}^{t}u_w{}^2\Delta\xi\right)$$

$$+\frac{2C_d}{n}R_h{}^{-1/3}S_0{}^{1/2}\left(\sum_{\xi=0}^{t}g\frac{\partial h}{\partial x}\Delta\xi^2 - gS_0t^2 + \frac{C_d}{n^2}R_h{}^{1/3}S_0t^2\right.$$

$$\left.-\frac{C_w\rho_a}{\rho_w R_h}\sum_{\xi=0}^{t}u_w{}^2\Delta\xi^2\right)$$

$$-\frac{C_d}{R_h}\left(\sum_{\xi=0}^{t}g\frac{\partial h}{\partial x}\Delta\xi - gS_0t + \frac{C_d}{n^2}R_h{}^{1/3}S_0t - \frac{C_w\rho_a}{\rho_w R_h}\sum_{\xi=0}^{t}u_w{}^2\Delta\xi\right)^2\Delta\xi$$

$$+\frac{\rho_a C_w}{\rho_w R_h}\sum_{\xi=0}^{t}u_w{}^2\Delta\xi$$

$$(3.34)$$

Which is approximate solution of Saint Venant equation (3.21) for computed velocity u (including water depth and wind speed), i.e. $u \approx u_2$

Therefore,

$$u \approx \frac{1}{n} R_h{}^{2/3} S_0{}^{1/2} - \frac{1}{n} R_h{}^{2/3} S_0{}^{1/2} \left(\sum_{\xi=0}^{t} g \frac{\partial^2 h}{\partial x^2} \Delta\xi^2 - \frac{2\rho_a C_w}{\rho_w R_h} \sum_{\xi=0}^{t} u_w \frac{\partial u_w}{\partial x} \Delta\xi^2 \right)$$

$$+ \left(\sum_{\xi=0}^{t} g \frac{\partial h}{\partial x} \Delta\xi^2 - g S_0 t^2 + \frac{C_d}{n^2} R_h{}^{1/3} S_0 t^2 \right.$$

$$\left. - \frac{C_w \rho_a}{\rho_w R_h} \sum_{\xi=0}^{t} u_w{}^2 \Delta\xi^2 \right) \left(\sum_{\xi=0}^{t} g \frac{\partial^2 h}{\partial x^2} \Delta\xi - \frac{2\rho_a C_w}{\rho_w R_h} \sum_{\xi=0}^{t} u_w \frac{\partial u_w}{\partial x} \Delta\xi \right)$$

$$- \left(\sum_{\xi=0}^{t} g \frac{\partial h}{\partial x} \Delta\xi - g S_0 t + \frac{C_d}{n^2} R_h{}^{1/3} S_0 t - \frac{C_w \rho_a}{\rho_w R_h} \sum_{\xi=0}^{t} u_w{}^2 \Delta\xi \right)$$

$$+ \frac{2 C_d}{n} R_h{}^{-1/3} S_0{}^{1/2} \left(\sum_{\xi=0}^{t} g \frac{\partial h}{\partial x} \Delta\xi^2 - g S_0 t^2 + \frac{C_d}{n^2} R_h{}^{1/3} S_0 t^2 \right.$$

$$\left. - \frac{C_w \rho_a}{\rho_w R_h} \sum_{\xi=0}^{t} u_w{}^2 \Delta\xi^2 \right)$$

$$- \frac{C_d}{R_h} \left(\sum_{\xi=0}^{t} g \frac{\partial h}{\partial x} \Delta\xi - g S_0 t + \frac{C_d}{n^2} R_h{}^{1/3} S_0 t \right.$$

$$\left. - \frac{C_w \rho_a}{\rho_w R_h} \sum_{\xi=0}^{t} u_w{}^2 \Delta\xi \right)^2 \Delta\xi + \frac{\rho_a C_w}{\rho_w R_h} \sum_{\xi=0}^{t} u_w{}^2 \Delta\xi$$

$$\tag{3.35}$$

If we do not consider any wind term in the momentum equation, the solution becomes

$$u \approx \frac{1}{n} R_h{}^{2/3} S_0{}^{1/2} - \frac{1}{n} R_h{}^{2/3} S_0{}^{1/2} \left(\sum_{\xi=0}^{t} g \frac{\partial^2 h}{\partial x^2} \Delta\xi^2 \right)$$

$$+ \left(\sum_{\xi=0}^{t} g \frac{\partial h}{\partial x} \Delta\xi^2 - gS_0 t^2 + \frac{C_d}{n^2} R_h{}^{1/3} S_0 t^2 \right) \left(\sum_{\xi=0}^{t} g \frac{\partial^2 h}{\partial x^2} \Delta\xi \right)$$

$$- \left(\sum_{\xi=0}^{t} g \frac{\partial h}{\partial x} \Delta\xi - gS_0 t + \frac{C_d}{n^2} R_h{}^{1/3} S_0 t \right)$$

$$+ \frac{2C_d}{n} R_h{}^{-1/3} S_0{}^{1/2} \left(\sum_{\xi=0}^{t} g \frac{\partial h}{\partial x} \Delta\xi^2 - gS_0 t^2 + \frac{C_d}{n^2} R_h{}^{1/3} S_0 t^2 \right)$$

$$- \frac{C_d}{R_h} \left(\sum_{\xi=0}^{t} g \frac{\partial h}{\partial x} \Delta\xi - gS_0 t + \frac{C_d}{n^2} R_h{}^{1/3} S_0 t \right)^2 \Delta\xi$$

$$(3.36)$$

Equation (3.36) is the approximate solution of Saint Venant equation given by Equation (3.21). Verification of this solution is presented in Chapter 4.

3.5 Computation of Thrust Force

Let u(x,t) denote the water velocity (computed by using water depth and wind speed as input) at spatial location x and temporal state t.

If a body travels along the curve x(t) through the fluid, the rate of change of velocity creates two kinds of accelerations: (a) Local acceleration and (b) Convective acceleration

The acceleration for fluid particle can be calculated by using

$$a = \frac{\partial u}{\partial t} + u \frac{\partial u}{\partial x} \qquad (3.37)$$

where, $\frac{\partial u}{\partial t}$ is called local acceleration i.e temporal variation and $u \frac{\partial u}{\partial x}$ is called convective acceleration when the particles move through regions with spatially varying velocity.

Since the water under consideration is moving, it is acted upon by external forces which will follow Newton's second law. i.e. F=ma

Therefore, the force for fluid dynamics can be calculated as

$$F = \rho A \left(\frac{\partial u}{\partial t} + u \frac{\partial u}{\partial x} \right) \qquad (3.38)$$

which can also be considered as the generated thrust force due to cyclone generated storm surge.

Using Equation (3.34), we can compute the local acceleration as

$$\frac{\partial u}{\partial t} \approx -\frac{1}{n}R_h{}^{2/3}S_0{}^{1/2}\left(\sum_{\xi=0}^{t}g\frac{\partial^2 h}{\partial x^2}\Delta\xi - \frac{2\rho_a C_w}{\rho_w R_h}\sum_{\xi=0}^{t}u_w\frac{\partial u_w}{\partial x}\Delta\xi\right) +$$

$$\left(\sum_{\xi=0}^{t}g\frac{\partial h}{\partial x}\Delta\xi^2 - gS_0 t^2 + \frac{C_d}{n^2}R_h{}^{1/3}S_0 t^2 - \right.$$

CwρaρwRhξ=0tuw2Δξ2ξ=0tg∂2h∂x2Δξ−2ρaCwρwRhξ=0tu
w∂uw∂xΔξ−g∂h∂x−gS0+Cdn2Rh13S0−CwρaρwRhuw2+2C
dnRh−13S012ξ=0tg∂h∂xΔξ2−gS0t2+Cdn2Rh13S0t2−Cwρa
ρwRhξ=0tuw2Δξ2−CdRhξ=0tg∂h∂xΔξ−gS0t+Cdn2Rh13S0t
−CwρaρwRhξ=0tuw2Δξ2

(3.39)

Using Equation (3.35), we can compute the convective acceleration as

$$
\begin{aligned}
\frac{\partial u}{\partial x} \approx -\frac{1}{n} R_h{}^{2/3} S_0{}^{1/2} &\left(\sum_{\xi=0}^{t} g \frac{\partial^3 h}{\partial x^3} \Delta\xi^2 - \frac{2\rho_a C_w}{\rho_w R_h} \sum_{\xi=0}^{t} u_w \frac{\partial^2 u_w}{\partial x^2} \Delta\xi^2 \right.\\
&- \frac{2\rho_a C_w}{\rho_w R_h} \sum_{\xi=0}^{t} u_w \left(\frac{\partial u_w}{\partial x}\right)^2 \Delta\xi^2 \Bigg)\\
&+ \left(\sum_{\xi=0}^{t} g \frac{\partial^2 h}{\partial x^2} \Delta\xi - \frac{2\rho_a C_w}{\rho_w R_h} \sum_{\xi=0}^{t} u_w \frac{\partial u_w}{\partial x} \Delta\xi \right) \left(\sum_{\xi=0}^{t} g \frac{\partial^2 h}{\partial x^2} \Delta\xi^2 \right.\\
&- \frac{2\rho_a C_w}{\rho_w R_h} \sum_{\xi=0}^{t} u_w \frac{\partial u_w}{\partial x} \Delta\xi^2 \Bigg)\\
&+ \left(\sum_{\xi=0}^{t} g \frac{\partial^3 h}{\partial x^3} \Delta\xi^2 - \frac{2\rho_a C_w}{\rho_w R_h} \sum_{\xi=0}^{t} u_w \frac{\partial^2 u_w}{\partial x^2} \Delta\xi^2 \right.\\
&- \frac{2\rho_a C_w}{\rho_w R_h} \sum_{\xi=0}^{t} u_w \left(\frac{\partial u_w}{\partial x}\right)^2 \Delta\xi^2 \Bigg) \left(\sum_{\xi=0}^{t} g \frac{\partial h}{\partial x} \Delta\xi - \sum_{\xi=0}^{t} g \frac{\partial z}{\partial x} \Delta\xi + \frac{C_d}{n^2} R_h{}^{1/3} S_0 \right.\\
&- \frac{C_w \rho_a}{\rho_w R_h} \sum_{\xi=0}^{t} u_w{}^2 \Delta\xi \Bigg) - \left(\sum_{\xi=0}^{t} g \frac{\partial^2 h}{\partial x^2} \Delta\xi - \frac{2\rho_a C_w}{\rho_w R_h} \sum_{\xi=0}^{t} u_w \frac{\partial u_w}{\partial x} \Delta\xi \right)\\
&+ \frac{2C_d}{n} R_h{}^{-1/3} S_0{}^{1/2} \left(\sum_{\xi=0}^{t} g \frac{\partial^2 h}{\partial x^2} \Delta\xi^2 - \frac{2\rho_a C_w}{\rho_w R_h} \sum_{\xi=0}^{t} u_w \frac{\partial u_w}{\partial x} \Delta\xi^2 \right)\\
&- \frac{2C_d}{R_h} \left(\sum_{\xi=0}^{t} g \frac{\partial h}{\partial x} \Delta\xi - \sum_{\xi=0}^{t} g \frac{\partial z}{\partial x} \Delta\xi + \frac{C_d}{n^2} R_h{}^{1/3} S_0 t \right.\\
&- \frac{C_w \rho_a}{\rho_w R_h} \sum_{\xi=0}^{t} u_w{}^2 \Delta\xi \Bigg) \left(\sum_{\xi=0}^{t} g \frac{\partial^2 h}{\partial x^2} \Delta\xi^2 - \frac{2\rho_a C_w}{\rho_w R_h} \sum_{\xi=0}^{t} u_w \frac{\partial u_w}{\partial x} \Delta\xi^2 \right)
\end{aligned}
$$

$$(3.40)$$

Now we can write Equation (3.38) as

$$F \approx \rho A \left[\left| \left\{ -\frac{1}{n} R_h^{2/3} S_0^{1/2} \left(\sum_{\xi=0}^{t} g \frac{\partial^2 h}{\partial x^2} \Delta\xi - \frac{2\rho_a C_w}{\rho_w R_h} \sum_{\xi=0}^{t} u_w \frac{\partial u_w}{\partial x} \Delta\xi \right) + \right. \right. \right.$$

$$\left(\sum_{\xi=0}^{t} g \frac{\partial h}{\partial x} \Delta\xi^2 - gS_0 t^2 + \frac{C_d}{n^2} R_h^{1/3} S_0 t^2 - \frac{C_w \rho_a}{\rho_w R_h} \sum_{\xi=0}^{t} u_w^2 \Delta\xi^2 \right) \left(\sum_{\xi=0}^{t} g \frac{\partial^2 h}{\partial x^2} \Delta\xi - \frac{2\rho_a C_w}{\rho_a R_h} \sum u_w \frac{\partial u_w}{\partial x} \Delta\xi \right) -$$

$$\left(g \frac{\partial h}{\partial x} - gS_0 + \frac{C_d}{n^2} R_h^{1/3} S_0 - \frac{C_w \rho_a}{\rho_w R_h} u_w^2 \right) + \frac{2C_d}{n} R_h^{-1/3} S_0^{1/2}$$

$$\left(\sum_{\xi=0}^{t} g \frac{\partial h}{\partial x} \Delta\xi^2 - gS_0 t^2 + \frac{C_d}{n^2} R_h^{1/3} S_0 t^2 - \frac{C_w \rho_a}{\rho_w R_h} \sum_{\xi=0}^{t} u_w^2 \Delta\xi^2 \right) -$$

$$\frac{C_d}{R_h} \left(\sum_{\xi=0}^{t} g \frac{\partial h}{\partial x} \Delta\xi - gS_0 t + \frac{C_d}{n^2} R_h^{1/3} S_0 t - \frac{C_w \rho_a}{\rho_w R_h} \sum_{\xi=0}^{t} u_w^2 \Delta\xi \right)^2 \right\} + u \left\{ -\frac{1}{n} R_h^{2/3} S_0^{1/2} \right.$$

$$\left(\sum_{\xi=0}^{t} g \frac{\partial^3 h}{\partial x^3} \Delta\xi - \frac{2\rho_a C_w}{\rho_w R_h} \sum_{\xi=0}^{t} u_w \frac{\partial^2 u_w}{\partial x^2} \Delta\xi^2 - \frac{2C_w \rho_a}{\rho_w R_h} \sum_{\xi=0}^{t} u_w \left(\frac{\partial u_w}{\partial x} \right)^2 \Delta\xi^2 \right) +$$

$$\left(\sum_{\xi=0}^{t} g \frac{\partial^2 h}{\partial x^2} \Delta\xi - \frac{2\rho_a C_w}{\rho_w R_h} \sum_{\xi=0}^{t} u_w \frac{\partial u_w}{\partial x} \Delta\xi \right) \left(\sum_{\xi=0}^{t} g \frac{\partial^2 h}{\partial x^2} \Delta\xi^2 - \frac{2\rho_a C_w}{\rho_w R_h} \sum_{\xi=0}^{t} u_w \frac{\partial u_w}{\partial x} \Delta\xi^2 \right) +$$

$$\left(\sum_{\xi=0}^{t} g \frac{\partial^3 h}{\partial x^3} \Delta\xi - \frac{2\rho_a C_w}{\rho_w R_h} \sum_{\xi=0}^{t} u_w \frac{\partial^2 u_w}{\partial x^2} \Delta\xi^2 - \frac{2C_w \rho_a}{\rho_w R_h} \sum_{\xi=0}^{t} u_w \left(\frac{\partial u_w}{\partial x} \right)^2 \Delta\xi^2 \right)$$

$$\left(\sum g \frac{\partial h}{\partial x} \Delta\xi + \frac{C_d}{n^2} R_h^{1/3} S_0 - \frac{C_w \rho_a}{\rho_w R_h} \sum_{\xi=0}^{t} u_w^2 \Delta\xi \right) - \left(\sum_{\xi=0}^{t} g \frac{\partial^2 h}{\partial x^2} \Delta\xi - \frac{2\rho_a C_w}{\rho_w R_h} \sum_{\xi=0}^{t} u_w \frac{\partial u_w}{\partial x} \Delta\xi \right) +$$

$$\frac{2C_d}{n} R_h^{-1/3} S_0^{1/2} \left(\sum_{\xi=0}^{t} g \frac{\partial^2 h}{\partial x^2} \Delta\xi^2 - \frac{2\rho_a C_w}{\rho_w R_h} \sum_{\xi=0}^{t} u_w \frac{\partial u_w}{\partial x} \Delta\xi^2 \right) - \frac{2C_d}{R_h}$$

$$\left(\sum_{\xi=0}^{t} g \frac{\partial h}{\partial x} \Delta\xi + \frac{C_d}{n^2} R_h^{1/3} S_0 t - \frac{C_w \rho_a}{\rho_w R_h} \sum_{\xi=0}^{t} u_w^2 \Delta\xi \right) \left(\sum_{\xi=0}^{t} g \frac{\partial^2 h}{\partial x^2} \Delta\xi^2 - \frac{2\rho_a C_w}{\rho_w R_h} \sum_{\xi=0}^{t} u_w \frac{\partial u_w}{\partial x} \Delta\xi^2 \right) \right\} \right]$$

<div align="right">(3.41)</div>

Where,

$$u \approx$$

$$\frac{1}{n} R_h{}^{2/3} S_0{}^{1/2} - \frac{1}{n} R_h{}^{2/3} S_0{}^{1/2} \left(\sum_{\xi=0}^{t} g \frac{\partial^2 h}{\partial x^2} \Delta \xi^2 - \frac{2\rho_a C_w}{\rho_w R_h} \sum_{\xi=0}^{t} u_w \frac{\partial u_w}{\partial x} \Delta \xi^2 \right) +$$

$$\left(\sum_{\xi=0}^{t} g \frac{\partial h}{\partial x} \Delta \xi^2 - g S_0 t^2 + \frac{C_d}{n^2} R_h{}^{1/3} S_0 t^2 - \right.$$

CwρaρwRhξ=0tuw2Δξ2ξ=0tg∂2h∂x2Δξ−2ρaCwρwRhξ=0tuw∂uw∂x
Δξ−ξ=0tg∂h∂xΔξ−gS0t+Cdn2Rh13S0t−CwρaρwRhξ=0tuw2Δξ+2Cd
nRh−13S012ξ=0tg∂h∂xΔξ2−gS0t2+Cdn2Rh13S0t2−CwρaρwRhξ=0
tuw2Δξ2−CdRhξ=0tg∂h∂xΔξ−gS0t+Cdn2Rh13S0t−CwρaρwRhξ=0t
uw2Δξ2Δξ+ρaCwρwRhξ=0tuw2Δξ

$$(3.42)$$

Equations (3.40) and (3.41) represent the thrust force due to momentum created by the wind and water mass. In present study, they are used to compute the thrust force exerted by the cyclone generated storm surge and are named as Dynamic Force Model (DFM).

Chapter 4

Model Verification, Calibration and Validation

4.1 Introduction

Calibration and validation are two important steps to assess model reliability. On the other hand, model verification is required to ensure a realistic solution of the model algorithms. One very simple interpretation of calibration is to adjust a set of parameters associated with a computational scheme so that the model agreement is maximized with respect to a set of experimental data (Trucano et al, 2006). Model validation is assigned to quantify our belief in the predictive capability of a model through comparison with a set of experimental data (Trucano et al., 2006). Uncertainty in both the measurement and the model are important and must be mathematically understood to correctly perform both calibration and validation. In this chapter, we intend to clarify the model reliability or a predictive modeling capability with verification, calibration and validation. Validation and calibration in Computational Science and Engineering both depend on results of verification. In this study, verification of DFM is performed by comparing the analytical solution of the model with a finite difference solution of the same governing equations. After setting the verified model parameters through calibration, DFM is validated by comparing the model generated velocity fields with the velocity field computed from the numerical solutions of Delft 3D dashboard and flow model.

4.2 Model Verification

In this study, a Dynamic Force Model (DFM) is developed by analytically solving the Saint-Venant Equations or 1D shallow water equations which are derived from Navier Stokes equations. This analytical solution is verified by comparing the analytical model results with the numerical solution. As described in Chapter 3, we use Variational Iteration Method as an analytical method. To verify this analytical solution, the numerical method selected is the Finite Difference Method. The reflexive condition is used as boundary conditions during the numerical solution. Using MATLAB, we have prepared two scripts for the analytical solution and the numerical solution respectively. During comparison, only the velocities from the DFM is compared with the numerical solution.

4.2.1 Numerical solution using finite difference method

Finite difference method is a reliable numerical method for the solutions of shallow water equation. The standard definition of finite difference method in elementary calculus is the following

$$\frac{\partial u}{\partial x} = \frac{u(x+\Delta x)-u(x)}{\Delta x} \text{ and } \frac{\partial u}{\partial t} = \frac{u(t+\Delta t)-u(t)}{\Delta t} \qquad (4.1)$$

In this study, the Saint-Venant equations (presented in Chapter 3) is solved by applying the finite difference method. The solution is given as:

$$u_i = \frac{u_{i-1}+u_{i+1}}{2} - \frac{1}{2\frac{dx}{dt}}(F_{i+1}-F_{i-1}) + \frac{S_{i+1}+S_{i-1}}{2}dt; \ \ i = 1,2,3,4,5,\ldots\ldots \qquad (4.2)$$

To verify the DFM code, the velocity field computed by Equation (4.2) is compared with the velocity field computed from DFM.

4.2.2 Hypothetical channel description

Wind blowing on a hypothetical channel of 5.1km long, 100m wide and 5m deep is considered for verification of the model which is shown in Figure 4.1. As no measured data is available, the model is verified indirectly by comparing the water velocity computed from the analytical solution of DFM with water velocity computed from a finite difference solution of the Saint-Venant equation (Equation 4.1). Steady and uniform state of flow represented by Manning's equation i.e. $u_0 = \frac{1}{n}R_h{}^{2/3}S_0{}^{1/2}$ is used as initial condition for this study(described in Chapter-3), where R_h is hydraulic redius and S_0 is bed slope for this channel.
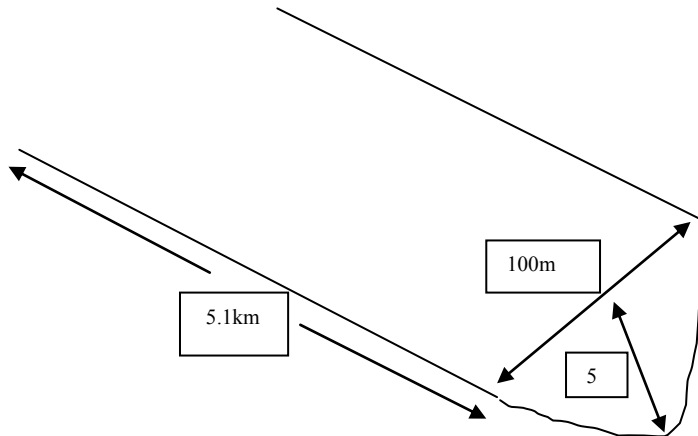
Figure-4.1: Hypothetical channel

DFM is verified by comparing with the numerical solution by constructing different cases. In Case-1, water depth and water surface slope are kept constant as shown in Figure-4.2. This results almost constant water velocity along the channel. Computed water velocity from the DFM and the numerical solution is shown in Figure-4.3. The result shows a perfect agreement between the DFM and the numerical solution.
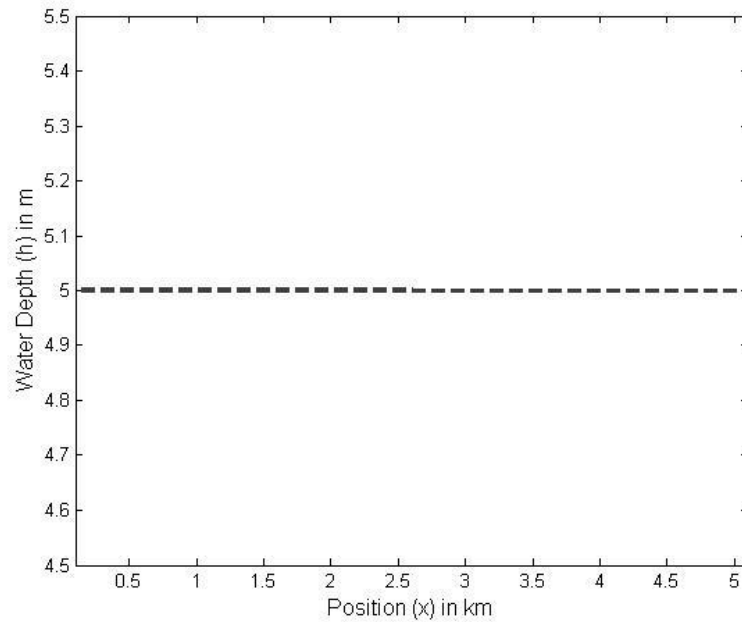
Figure-4.2: Water depths h(m) in different positions x(km) along horizontal.
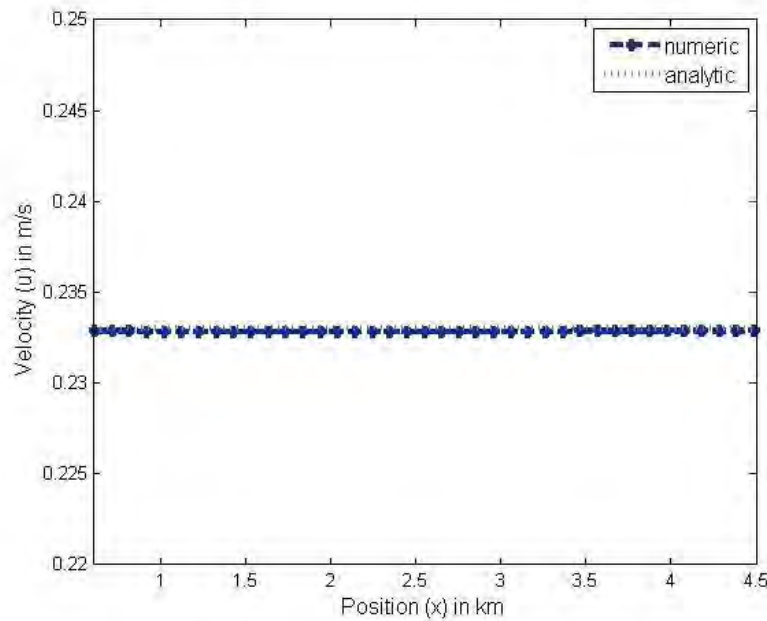
Figure-4.3: Comparison of longitudinal velocity profile u(m/s) between the DFM and the numerical solution.

In Case-2, water depth is varying along the channel as shown in Figure-4.4. This results variable water slope. Comparison of computed water velocity between the DFM and the numerical solution is shown in Figure-4.5. The result shows a perfect agreement between the DFM and the numerical solution.
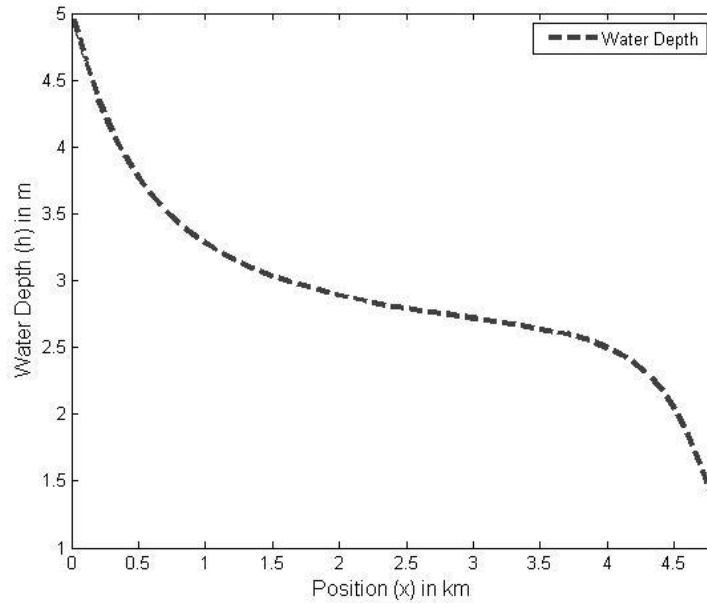
Figure-4.4: Water depths h(m) in different positions x(km) along horizontal.
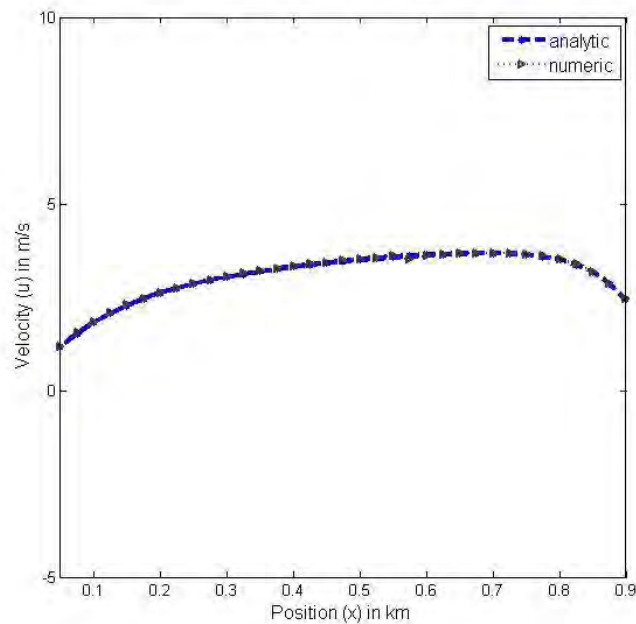
Figure-4.5: Comparison of longitudinal velocity profile u(m/s) between the DFM and the numerical solution.

In Case-3, wind speed term is included in the momentum equation. Hypothetical wind with variable speed is exerted on the surface of the channel as shown in Figure-4.6. Comparison of water velocity between the DFM and the numerical solution is shown in Figure-4.7. The result shows a reasonable agreement between the DFM and the numerical solution.
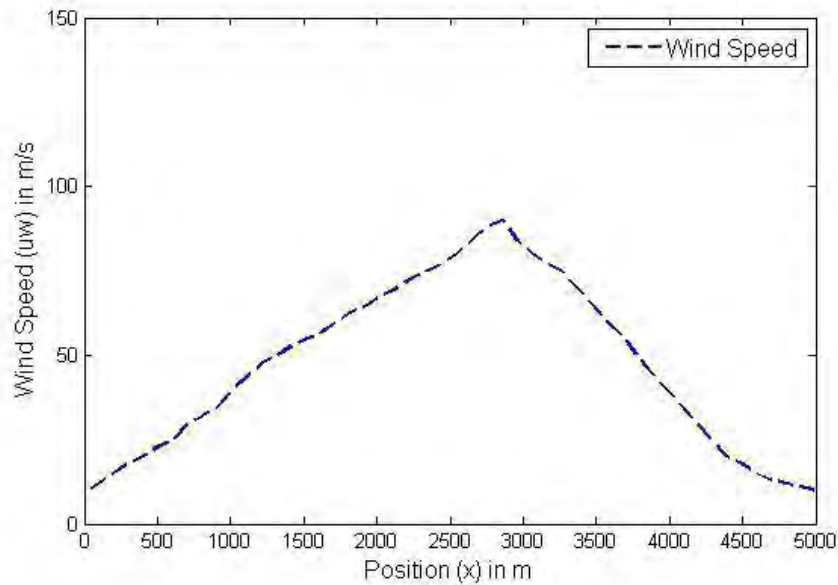
Figure-4.6: Variable wind Speed u_w(m/s) in different positions x(m) along the channel.
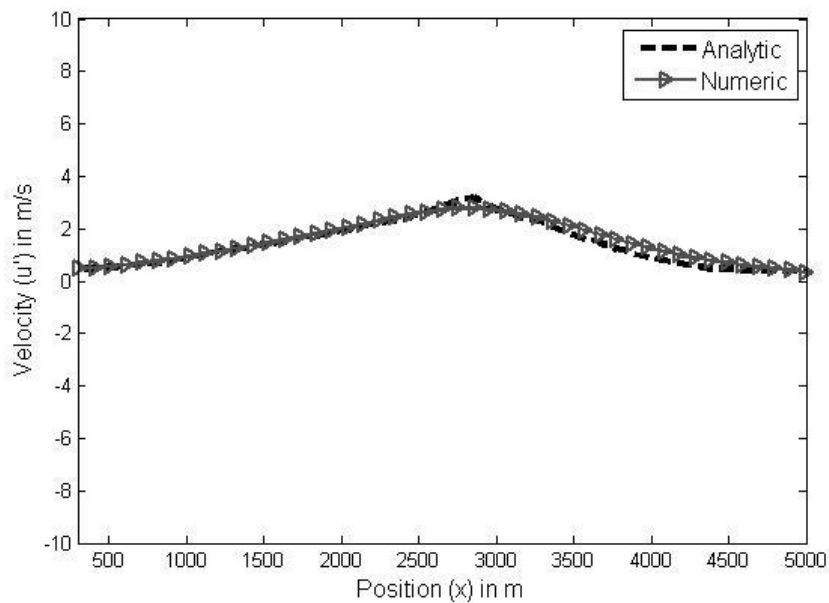
Figure-4.7:Comparison of longitudinal velocity profile u(m/s) between the DFM and the numerical solution.

4.3 Calibration of the Model

For calibrating the DFM we used wind drag coefficient as the calibration parameter. The model is calibrated for wind drag coefficient after selecting the wind and cyclone track. The transfer of momentum by atmosphere to the ocean produces a wave field that imposes shear stress which ultimately causes the rise of water level (Powell et al, 2003) and results inundation in the coastal lands. The drag coefficient C_d controls the transfer of momentum from wind to water surface in the governing storm tide equations (Noble and Hendricson, 1974). It depends on factors such as the wind speed, wave height and direction, and air temperature. In modeling storm surge, this coefficient is a crucial parameter for estimating the surge height (Drews, C, 2013). Different fields experiments and numerical methods have been carried out in the past few decades to predict the wind drag coefficient, thus to compute the resulting wind stress initiated by cyclonic winds. But there is always a controversy on the range of wind drag coefficient for specific regions and its linear relationship with the associated wind speed. Studies from 1970 to 1980 (Charnock, 1955; Large et al., 1981; Smith et al., 1975) suggested that the magnitude of this coefficient increases to a good approximation linearly with increasing wind speed. Smith (Smith et al, 2005) indicated that the drag coefficient continues to increase with wind speed, at least up to 21m/s which was later supported by Garret, 1977. On the other hand, recent studies (Bender, 2007; Kim et al., 2008; Kohno and Kigaki, 2006) recommended that the magnitude of the coefficient is either constant or increase monotonically with increasing surface wind speed. Zhizhua (2010) indicated that increase of the drag coefficient with the increase of wind speed up to 40 m/s followed by a decrease with further increase of wind speed. In present study, it is found that the magnitude of wind drag coefficient increases with wind the increasing wind speed which is shown in figure 4.8.
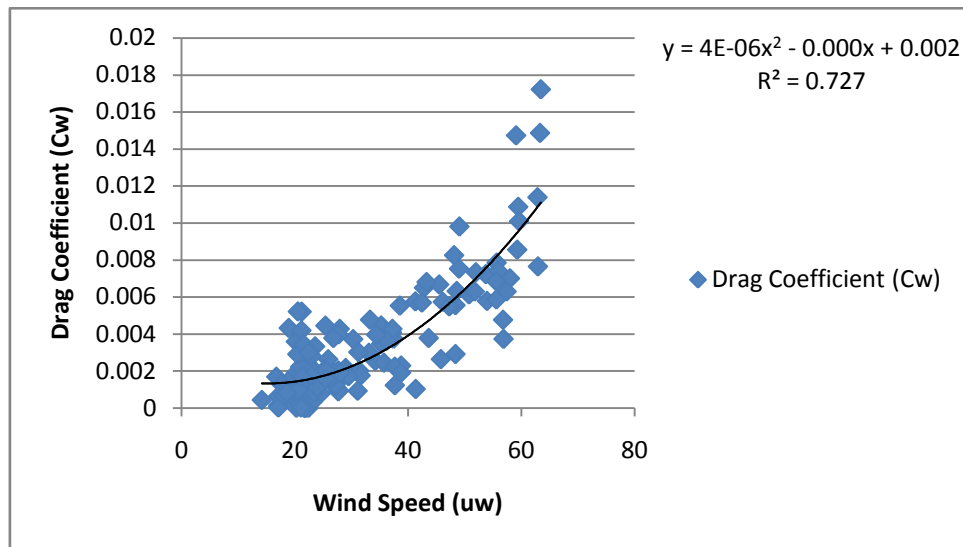
Figure 4.8: Increment of Drag coefficient with wind speed.

4.4 Validation of the Model

Validation of DFM is performed from two different approaches. These are:

1. Validation with the tsunami data (Murata et al., 2011).
2. Validation of the flow field of DFM with numerical model (Delft 3D) results.

4.4.1 Validation with the tsunami data

Tsunami is a natural disaster which is a long, high sea wave caused by an earthquake or other disturbance. A study on tsunami was done in Japan(Murata et al, Imamura et al, Katoh et al, Kawata et al, Takahashi et al and Takayama et al, 2011). They evidenced that the drag force F_d acting on buildings, etc is assumed to be proportionate to the square of the flow velocity and can be estimated by the following equation:

$$F_d \cong 0.61\gamma_w C_d h^2 B \qquad (4.3)$$

Where, γ_w is the weight of seawater per unit of volume, C_d is a drag force coefficient and B is the breadth of a building in the flow direction. Table 4.1 shows the values recommended for the water velocity and the resultant force that will cause damage to different degrees for specific type of structures.

Chapter 4: Model Verification, Calibration and Validation

Table 4.1: Standards for judging degree of damage by type of construction for Tsunami

	Moderate Damage		Heavy Damage	
Type of Construction	u (m/s)	F (kN/m)	u (m/s)	F(kN/m)
Concrete block	6.0	60.5~110	9.1	329~598
Wood	4.2	15.1~27.5	4.5	26.9~48.9

In the present study, values of forces exerted by surge water is computed by DFM and results are presented in Table 4.2.

Table 4.2: Standards for judging degree of damage by type of construction due to Storm Surge

	Moderate Damage		Heavy Damage	
Type of Construction	u (m/s)	F (kN/m)	u (m/s)	F(kN/m)
Concrete block	6.0	70.5~115	9.1	400~598
Wood	4.2	20.1~30.5	4.5	30.9~50.0

The force thus computed from the DFM is compared with the tsunami data and results are shown in Table 4.3. Table 4.3 shows that although tsunami does not have any wind component, the resultant force from tsunami is comparable to that from the cyclone generated storm surge. In this specific example, the force of storm surge computed by DFM is within 4% to 19% deviated from the tsunami generated force.

Table 4.3: Comparison between DFM data and tsunami data.

Type of Construction	Moderate Damage				Heavy Damage			
	u (m/s)	Tsunami data, F (kN/m)	DFM data, F (kN/m)	Deviation	u (m /s)	Tsunami data, F (kN/m)	DFM data, F (kN/m)	Deviation
Concrete block	6	60.5~110	70~115	9.5%	9.1	329~598	400~620	9%
Wood	4.2	15.1~27.5	20~30.5	19%	4.5	26.9~48.9	30~50.0	4.18%

4.4.2 Validation of the flow field of DFM with numerical model (Delft 3D) results

Study area for this part comprises the coastal area (covers an area from the shore to 37 to 195 kilometers inland) of Bangladesh (Islam, R., 2006) which constitutes 19 out of the total 64 districts of the country (Figure 2) and 153 upazilas (second lowest regional administrative unit). Among them 12 districts and 51 upazilas are severely affected by the cyclone induced storm surge (Islam, R., 2006).
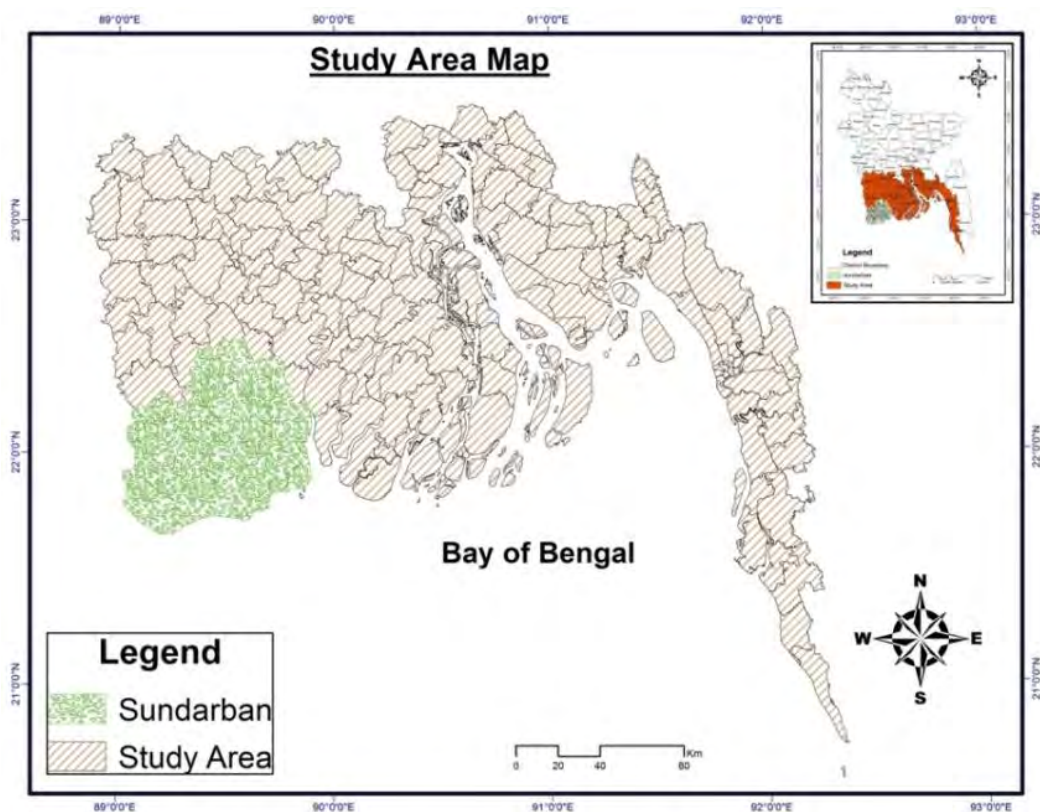
Figure 4.9: Study Area for validation of Dynamic Force Model

DFM is applied in this study region to compute the flow field. In doing this, the required water depth and wind speed for the DFM is extracted from the Delft 3D dashboard and flow model (Sakib et al, 2015; Nihal et al, 2015; Haque et al, 2015; Rahman et al, 2015). The computed flow field thus computed from the DFM is compared with the flow field computed from the Delft 3D and the comparison is shown in Figure 4.10.
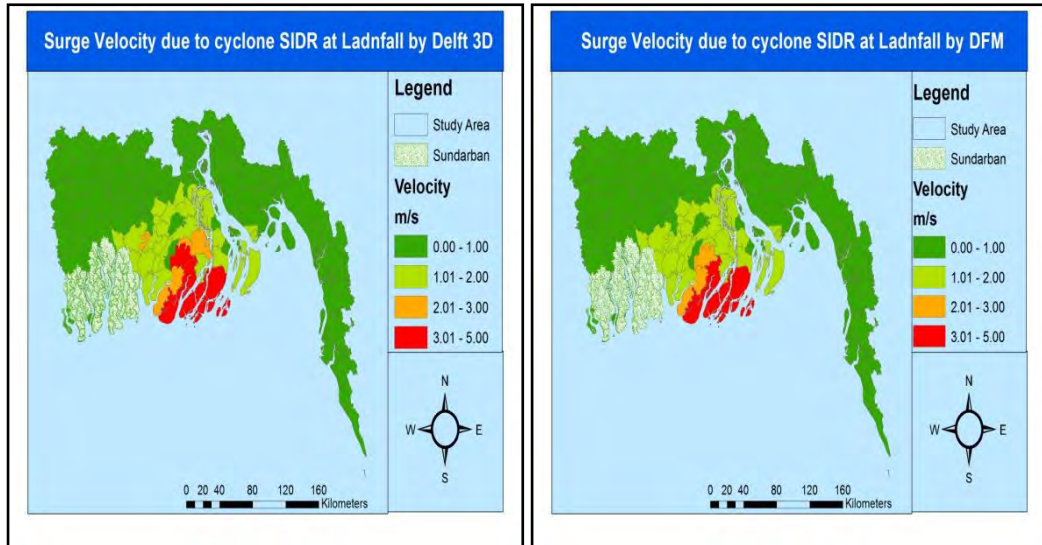
Figure 4.10: Quantitative and Visual Comparison of two maps for flow fields from Dynamic Force Model and Delft 3D Model.

To quantify the visual qualitative color comparison, a one-to-one function is defined among the colors between the two maps. In this way, it is possible to quantify the overlap color and deviated color between the two maps. The overlap color shows the similarity and the deviated color shows the dissimilarity between the maps. The comparison is shown in Table 1. The comparison shows that surge velocities computed with DFM is 97% similar to that computed with Delft3D. It is noted here that Delft3D is a validated storm surge model in the coastal zone of Bangladesh (Sakib et al., 2015; Nihal et al., 2015).

Table 4.1: Map Comparison

Models	In Percentage (%)	
	Overlapped Colors	Deviated Colors
Delft3D – DFM	97%	3%

Chapter 5

Model Application

5.1 Introduction

In this study, Dynamic Force model (DFM) described in Chapter-3 and validated in Chapter-4 is applied in the coastal zone of Bangladesh. The DFM is applied to compute the distributive thrust forces for the following events (1) Cyclone SIDR (2) 1991 cyclone (3) Hypothetical SIDR-like cyclone (4) Impact of Sunadarban (5) Impacts of coastal afforestation (6) Impacts of coastal embankments.

5.2 Thrust Force due to Cyclone SIDR

Cyclone SIDR is considered one of the devastating cyclone that made landfall at the east of Sundarban. During the time of landfall, the maximum wind speed of this cyclone was 227km/hr. This cyclone is believed to generate a surge depth of 7.6m. Computed thrust force due to cyclone SIDR at the time of landfall is shown in Figure 5.1.Table 5.1 shows the maximum thrust force at different coastal districts of Bangladesh due to cyclone SIDR.

Table 5.1: Maximum thrust force at different districts of coastal zone due to SIDR.

District	Maximum thrust force (F) in kN/m
Bagerhat	23.12283
Barguna	50.75592
Barisal	17.20786
Bhola	58.2356
Jhalokati	13.43796
Khulna	3.55096
Patuakhali	138.9503
Pirojpur	21.21142
Satkhira	2.196654

Cyclone SIDR hit the coastal districts of Patuakhali, Barguna, Jhalokati and Pirojpur of Bangladesh. Most areas of Patuakhali and Bhola is situated at the east of the cyclone track. Thrust force is found to be the maximum at Patuakhali district and second in Bhola

district. This is due to the fact that cyclone causes major impact at east of a cyclone track (right side of cyclone track in the northern hemisphere). Khulna and Satkhira is situated at the left side of the cyclone track. For this reason, thrust forces are found very small in these districts.
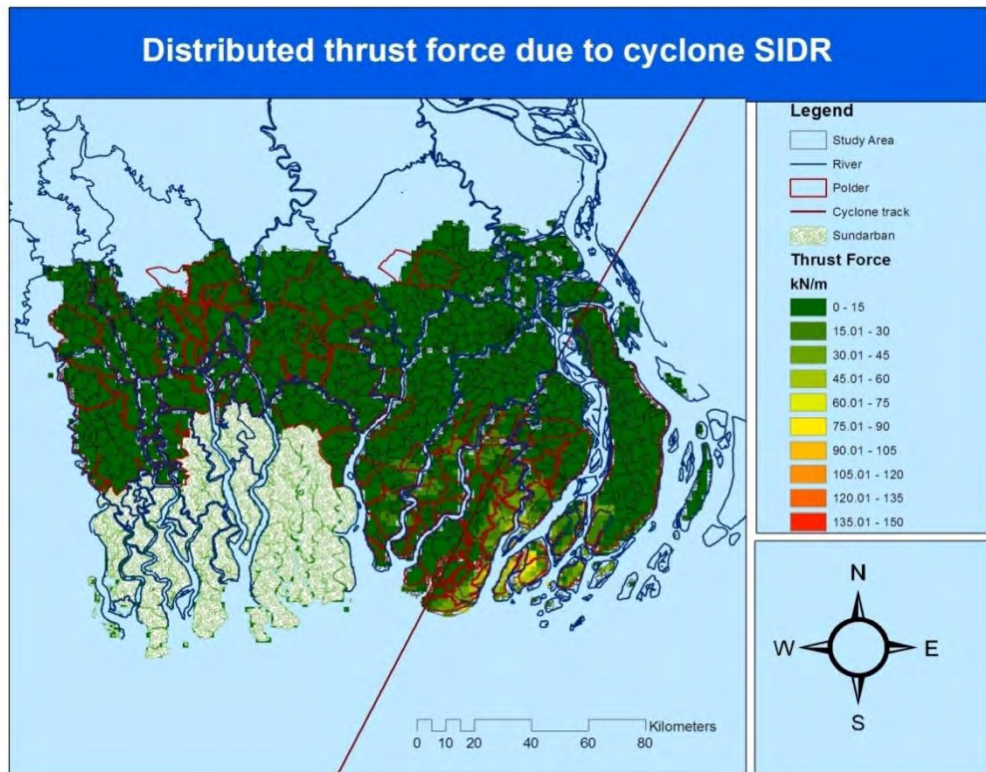
Figure 5.1: Distributed thrust force due to cyclone SIDR at landfall in the coastal zone of Bangladesh

5.3 Thrust Force due to 1991 Cyclone

In recent past, 1991 cyclone is the deadliest cyclone (except the 1970 Bhola cyclone which has limited data to model) that made landfall on Bangladesh coast. This cyclone made landfall on the Chittagong coast. At the time of landfall, 1991 cyclone has the maximum wind speed of 198km/hr with an estimated surge depth of 7.4m. The DFM is applied to compute the thrust force at the time of landfall and the results are shown in Figure 5.2 and in Table 5.2.

Table 5.2: Maximum thrust force at different districts of coastal zone due to 1991 cyclone.

District	Maximum thrust Force (F) in kN/m
Bagerhat	0.695824
Barguna	0.91635
Barisal	1.484596
Bhola	4.375396
Chandpur	0.981675
Chittagong	54.66853
Cox'S Bazar	30.98913
Feni	3.986283
Gopalganj	0.205914
Jessore	0.045367
Jhalokati	0.324584
Khulna	0.482359
Lakshmipur	4.572701
Narail	0.202916
Noakhali	20.6813
Patuakhali	2.3012
Pirojpur	1.011592
Satkhira	0.923845
Shariatpur	0.71964

1991 cyclone hits the coastal district of Chittagong and thrust force is found to be the maximum at Chittagong. The second highest thrust force is in Cox's bazar because it is situated at the right side of the cyclone track. Other districts which are situated at the left side of cyclone track experienced very low thrust force.
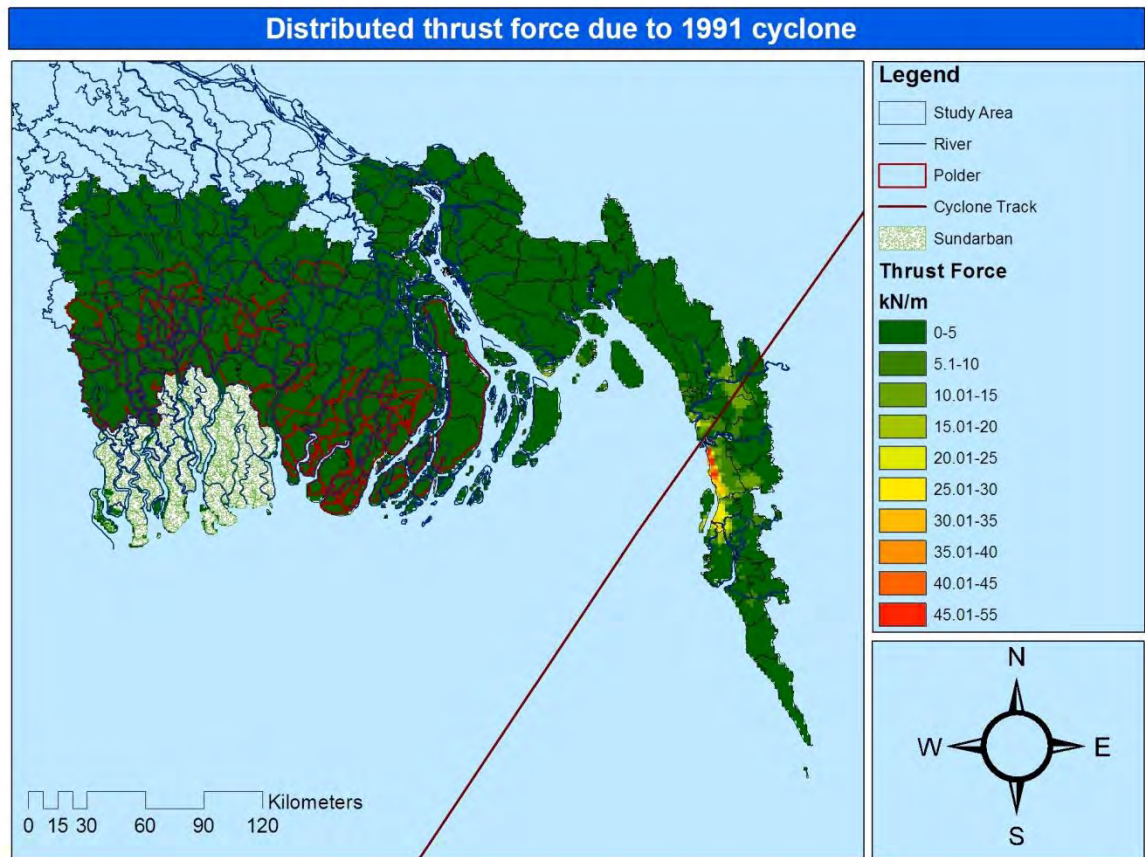
Figure 5.2: Distributed thrust force due to 1991 cyclone at landfall in the coastal zone of Bangladesh

5.4 Hypothetical SIDR-like Cyclone

By SIDR-like cyclones, we mean cyclones which has similar intensity as that of SIDR but has a different landfall location. In this case, it is assumed that the SIDR-like cyclone has a landfall location at the mouth of Lohalia river (actual SIDR made landfall on the east side of Sundarban). This location is similar to the location of 1970 Bhola cyclone which is believed to be one of the most devastating cyclone on Bangladesh coast. Computed thrust force by applying the DFM is shown in Figure 5.3 and in Table 5.3.

Table 5.3: Maximum thrust force at different districts of coastal zone due to hypothetical SIDR like cyclone.

District	Thrust Force (F) in kN/m
Bagerhat	17.94382
Barguna	37.33977
Barisal	16.9637
Bhola	104.4294
Jhalokati	11.98503
Khulna	2.848184
Patuakhali	137.0111
Pirojpur	14.23482
Satkhira	1.343622

Hypothetical SIDR like cyclone makes landfall at the mouth of Lohalia river. Two coastal districrs namely Patuakhali and Bhola are situated near the Lohalia river. As expected, thrust forces are found to be the maximum at Patuakhali and Bhola.
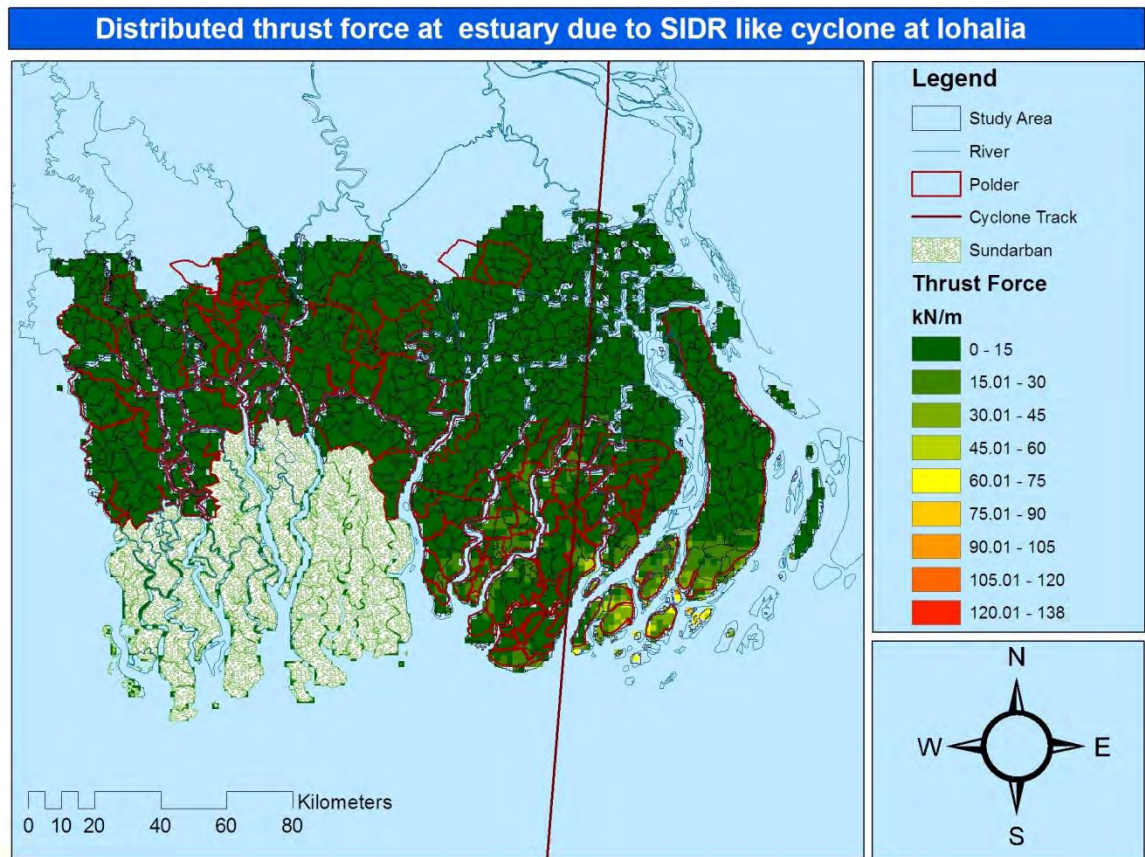
Figure 5.3: Distributed thrust force at estuary due to SIDR like cyclone at lohalia.

5.5 Impact of Sundarban on Distributive Thrust Force

Sundarban, the largest mangrove forest in the world, is known to act as a buffer against the cyclone and storm surge. Theoretically, Sundarban absorbs the initial thrust of the wind and acts to ―resist‖ the storm surge flooding. The role of Sundarban was evident during the cyclone SIDR when the Sundarban solely defended the initial thrust of the cyclonic wind and the resulting storm surge inundation. In doing this, Sundarban sacrificed 30% of its plant habitats. Studies show that Sundarban generally acts as a buffer against the storm surge when landfall of the cyclone is at or close to the Sundarban (Sakib et al., 2015). In this application of DFM, cyclone SIDR is considered in its actual landfall location (east of Sundarban) and in a hypothetical landfall location (exactly at the Sundarban) to study the role of Sundarban as a buffer against thrust force during the passage of cyclone generated storm surge.

Computed thrust force by using DFM is shown in figure 5.4 and in Table 5.4.

41
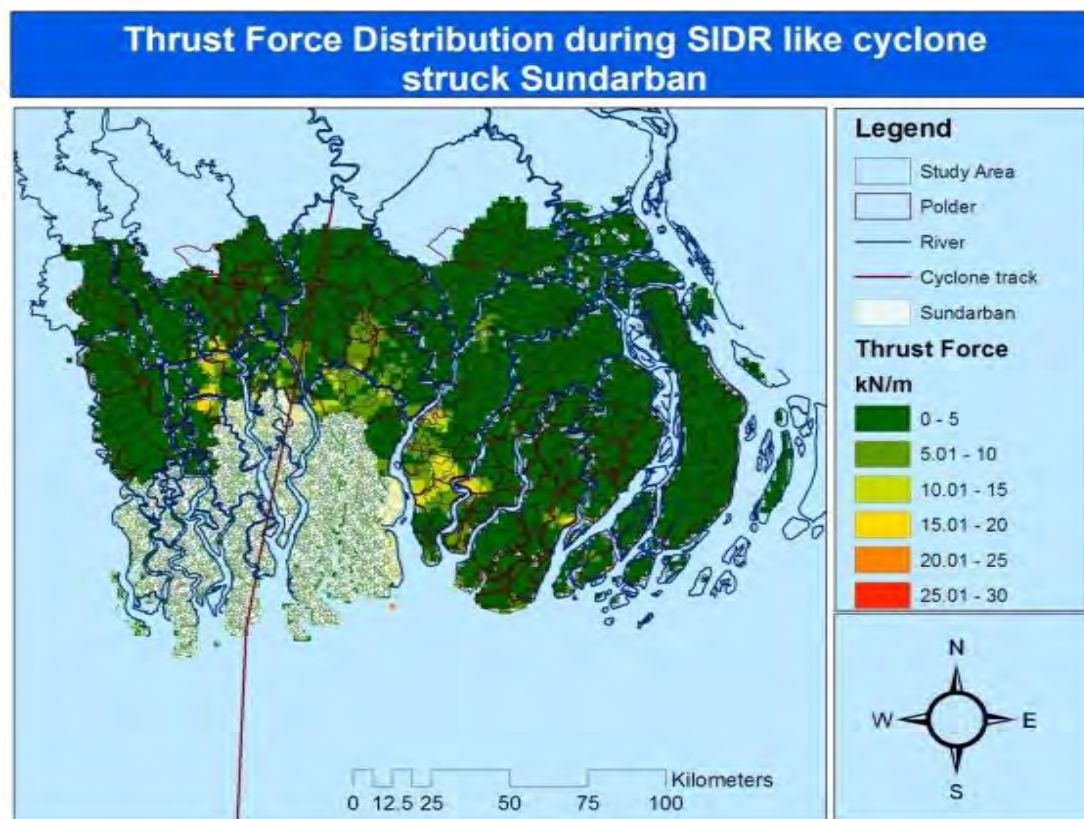
Figure 5.4: Distributed thrust force due to hypothetical SIDR like cyclone at Sundarban.

Table 5.4: Maximum thrust force at different districts of coastal zone due to hypothetical SIDR like cyclone at Sundarban

District	Maximum thrust force (F) in kN/m due to hypothetical SIDR like cyclone hits at Sundarban
Bagerhat	23.10415
Barguna	21.55399
Barisal	4.820411
Bhola	3.937712
Jhalokati	6.036051
Khulna	26.25247
Patuakhali	17.57269
Pirojpur	16.49162
Satkhira	9.603802

For this cyclone, the maximum thrust force is found to be 26kN/m at Khulna. Table 5.1 shows the thrust force distribution due to cyclone SIDR when its landfall location is in the

east of Sundarban (actual SIDR). The maximum thrust force due to actual SIDR is found to be 138kN/m at Patuakhali. Comparing hypothetical-SIDR (Table 5.3) and actual-SIDR(Table 5.1), it is found that the maximum thrust force during actual-SIDR (not directly influenced by Sundarban) is reduced by about 81% during hypothetical-SIDR (directly influenced by Sundarban). This shows the buffering capacity of Sundarban in reducing the thrust force.

5.6 Impacts of Coastal Afforestation on Distributive Thrust Force

Coastal afforestation has been widely recognized as a natural method to reduce the energy of storm surges (Rahman and Rahman, 2013). In this application of DFM, a 1km wide of coastal belt of Bangladesh is assumed to be covered by planted afforestation (Figure 5.5). This planted afforestation is considered in addition to the existing natural mangrove forest, the Sundarban. Two cyclones with the strengths of SIDR are assumed to make landfall on two different locations along this afforested coast (Figure 5.5). These are: (a) + (b) Cyclone SIDR makes landfall at the mouth of Lohalia river.
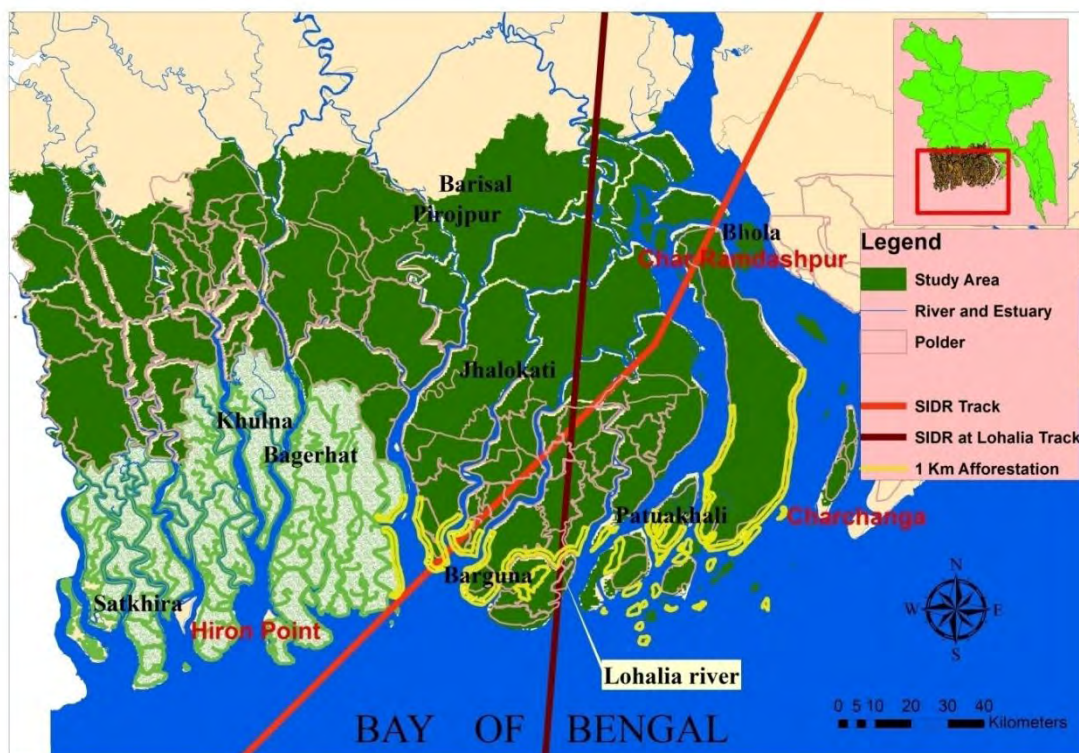
Figure 5.5: Coastal region of Bangladesh with Sundarban and planted afforestation.

For actual landfall location of SIDR

The DFM is applied to compute distributive thrust force by considering landfall of cyclone SIDR in its actual location but in an afforested coast. Comparison of maximum thrust force in different coastal districts are shown in Figure 5.6 and in Table 5.5.

Table 5.5:Comparison of maximum thrust forces between 'with afforestation' and 'without afforestation' during actual SIDR .

District	Maximum thrust force (F) in kN/m without afforestation	Maximum thrust force (F) in kN/m with afforestation
Patuakhali	115	75.45
Bhola	58.2356	42.2356
Barguna	50.75592	40.75592
Bagerhat	23.12283	20.12283
Pirojpur	21.21142	18.21142
Barisal	17.20786	9.20786
Jhalokati	13.43796	6.43796
Khulna	3.55096	1.55096
Satkhira	2.196654	0.196654

As shown in Table 5.5, the maximum thrust force for ‗without afforestation' is found to be 115kN/m at Patuakhali district which is reduced to 39kN/m with the introduction of afforestation (66% reduction). This shows the buffering capacity of coastal afforestation against the storm surge induced thrust force.
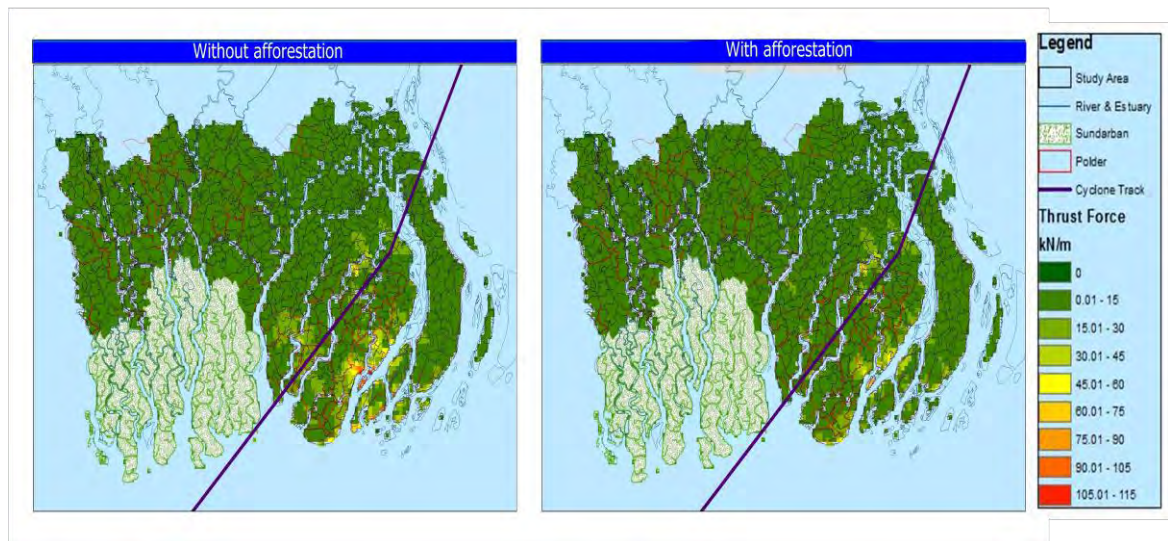
Figure 5.6: Comparison of thrust force due to cyclone SIDR in its actual landfall location for 'with' and 'without' afforestation

For Lohalia mouth landfall location of SIDR

In this case, SIDR is made to fall on land at the mouth of the Lohalia estuary. This specific application is studied for two reasons. One is to consider a landfall location which is considered to be vulnerable for Bangladesh coast (remembering the fact that this is the landfall location of 1970 Bhola cyclone). The other is to consider a landfall location which is far away from the Sundarban (natural mangrove forest). Computed thrust force due to this cyclone and comparison of the similar case when there is no afforestation is shown in Figure 5.7 and in Table 5.6.

Table 5.6: Comparison of maximum thrust forces between 'with afforestation' and 'without afforestation' during SIDR like cyclone at Lohalia river.

District	Maximum thrust Force (F) in kN/m without afforestation	Maximum thrust Force (F) in kN/m with afforestation
Patuakhali	105	65.0111
Bhola	95.4294	55.4294
Barguna	37.33977	33.75592
Bagerhat	17.94382	14.12283
Barisal	16.9637	13.21142
Pirojpur	14.23482	9.20786
Jhalokati	11.98503	6.43796
Khulna	2.848184	1.55096
Satkhira	1.343622	0.196654

Table 5.6 shows that the maximum thrust force in the case for ‗without afforestation‗ is 105kN/m which is reduced to 65kN/m (37% reduction) for ‗with afforestation‗. At Bhola, the afforestation has reduced the thrust force from 95kN/m to 55kN/m (42% reduction).

If Tables 5.3, 5.4 and 5.5 are compared, it is found that buffering capacity of Sundarban is more than buffering capacity of artificial afforestation (Sundarban reduces the maximum thrust force by approximately 81% while the artificial afforestation reduces the maximum thrust force by 37% to 66%). This is expected in the sense that Sundarban covers a much

wider area compared to the artificial afforestation. This implies that increasing the widths of artificial afforestation will also increase its buffering capacity.
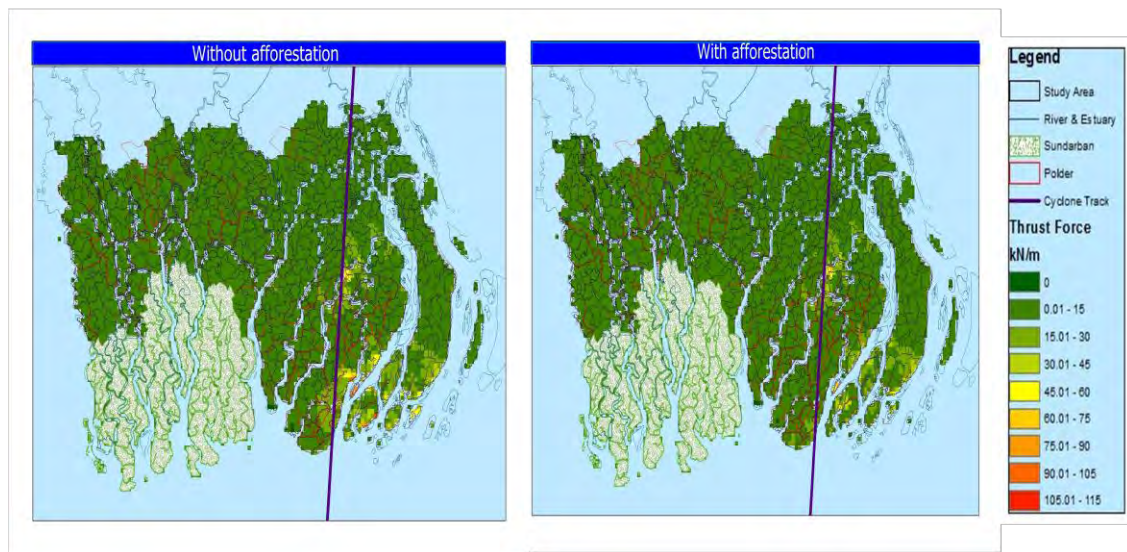
Figure 5.7: Comparison of thrust force due to cyclone SIDR when its actual landfall location is at the mouth of Lohalia estuary for 'with' and 'without' afforestation.

5.7 Impacts of Coastal Embankments on Distributive Thrust Force

Embankments in Bangladesh coast is a type of encircled structure for a certain location and is known as ‗polder' (a dutch word). These polders are built to protect the enclosed areas from tidal and storm surge flooding. In this application of DFM, impact of these polders on thrust force is studied. This application shows capability of DFM to compute the thrust force in an enclosed area (protected land) where surge water cannot enter. So, thrust force in these areas are generated only due to cyclone wind (in the non-protected area thrust force is generated due to combined action of cyclone wind and surge water).

To compare the impact of polder on the thrust force, one specific area in the coast (6 unions of Kuakata, Lata Chapli, Kalapara and Kathalia upazila in Patuakhali district) is considered which is affected by cyclone SIDR. This specific area is originally ‗poldered' (protected land). To study the polder impact, the polder is artificially removed from the area (the protected land becomes non-protected land).By applying the Delft3D numerical model (Sakib et al., 2015),inundation due to storm surge of the area as ‗protected land' and ‗non-protected land' is simulated and is shown in Figure 5.8. Inundation is simulated to show the combined impact of ‗cyclone wind & surge wave' and ‗cyclone wind only' on

the distributive thrust force. As expected, when there is polder, the area is not inundated. After removal of the polder, the area gets inundated.
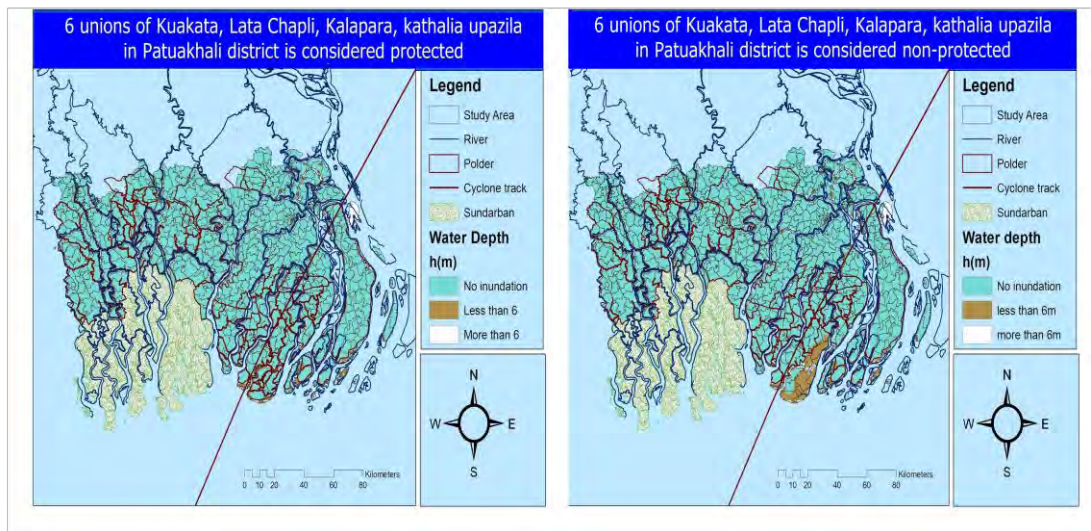
Figure 5.8: Inundation conditions at 6 unions of Kuakata, Lata Chapli, Kalapara, Kathalia upazila in Pattuakhali district of Bangladesh when the areas are considered either protected (left figure) or non-protected (right figure) due to a SIDR like cyclone.

The DFM is then applied in these two situations and the results are shown in Figure 5.9. Computed values of thrust force in this specific area for ‗with protected' and ‗without protected' condition is shown in Table 5.6.
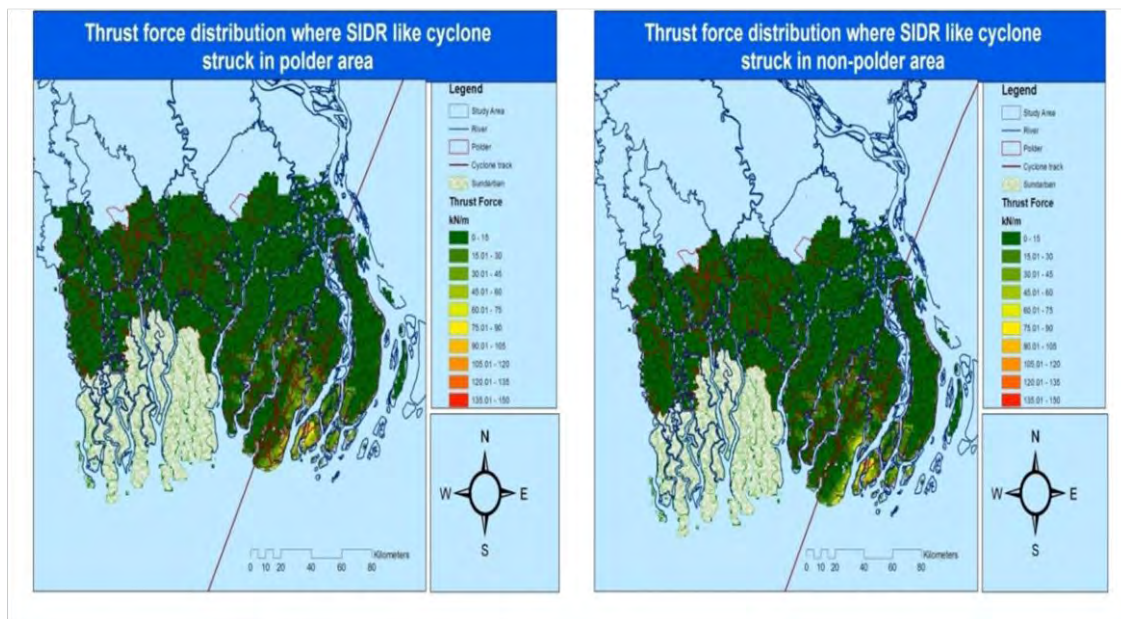
Figure 5.9: Thrust force distribution at 6 unions Kuakata, Lata Chapli, Kalapara, kathalia upazila in Pattuakhali districts of Bangladesh when the areas are considered either protected (left figure) or non-protected (right figure) due to a SIDR like cyclone.

Table 5.7: Comparison of the maximum thrust force at each union of Kuakata, Lata Chapli, Kalapara, kathalia upazila in Pattuakhali districts of Bangladesh when the areas are considered either protected or non-protected

Union	When protected	When non-protected
	Maximum Force (F) in kN/m	Maximum Force (F) in kN/m
Dhankhali	58.84	80.03
Dhulasar	60.38	74.42
Lalua	66.59	89.96
Lata Chapli	34.51	41.77
Mithaganj	53.39	62.84
Tiakhali	14.89	15.51

Figure 5.9 and Table 5.6 show that when the area is protected, the thrust forces are much smaller compared to the situation when the area is non-protected. In protected condition, the thrust force is due to the momentum created by the *'cyclone wind only'*. In non-protected condition, the thrust force is due to the combined impact of momentum created by the *'cyclone wind & water mass of the surge wave'*. The results show that the thrust force due to *'cyclone wind only'* is much less than the thrust force due to the combined impact of _*cyclone wind & surge wave'*. The results also show the ability of DFM to compute the thrust force due to *'wind only'* and due to the combined impact of *'wind & surge'*.

Chapter 6

Conclusion

6.1 Conclusion

Tropical cyclones associated with storm surges produce force generated by the momentum of cyclone winds and huge mass of moving surge waves. This force can damage or destroy buildings, bridges, roads, overpasses, personal property and other outside objects. These damages cause in economic losses to a region and may affect large number of population globally.

Cyclone generated storm surge is a frequent phenomenon along Bangladesh coast. Casualties and damages from cyclones in Bangladesh are caused by forces generated by cyclone winds and storm surges. Till today, no attempt is made to quantify this force. Once quantified, this force can be used to assess impacts of a cyclone on coastal infrastructure.For example, computed thrust force can be used to determine fate of a housing (pacca, semi-pacca, katcha or jhupri) during the passage of a cyclone over a populated area.

In this study, a Dynamic Force Model (DFM)is developed by analytically solving the Saint-Venant equations derived from Navier-Stokes equations. The model computes the distributive thrust force which is generated by the cyclonic wind and moving surge. As an analytical method, Variational Iteration Method (VIM) is used to solve the equations. During solution, steady and uniform state of flow computed by Manning's equation is considered as an initial condition. Thrust force is computed from local and convective accelerations of moving water dynamics.

The model is verified by applying the model in a hypothetical channel on which wind is blowing. The computed water velocity by analytical solution is compared with a finite difference solution and reasonable agreement is found. Wind drag coefficient is used as the calibration parameter. It is found that wind drag coefficient increases with the increase of wind speed. Flow field of DFM is validated by comparing the surge velocity computed

by DFM with the surge velocity computed by a numerical model Delft3D. The coastal zone of Bangladesh is selected as the study area during model validation.

After verification, calibration and validation – the DFM is applied in the coastal zone of Bangladesh. The model computes distributive thrust force in the entire coastal zone for cyclone SIDR, 1991 cyclone and a hypothetical SIDR-like cyclone. The model is also applied to compute the impacts of Sundarban and artificial coastal afforestation in reducing the surge generated thrust force. To show the capability of the model to differentiate the impact of ‗cyclone wind only' and impacts of ‗cyclone wind & surge wave' – a separate application of the model is made in a protected area. Following results are found from these applications:

a. For all the cyclones, maximum impact of thrust force is found to be at the right side of the cyclone track.

b. For cyclone SIDR (wind speed of 227km/hr), the maximum thrust force of 138 kN/m is found at Pataukhali district. For a cyclone that has similar strength of SIDR but has a landfall east of SIDR (at the mouth of Lohalia river), location of the maximum thrust force remains in the Patukhali district with almost similar magnitude (137 kN/m). For 1991 cyclone (wind speed of 198 km/hr) the maximum thrust force of 54 kN/m is found in Chittagong district. This shows that magnitude of thrust force depends on the wind speed in addition to the surge wave.

c. Sundarban as a buffer to reduce the magnitude of thrust is found to be effective. For a SIDR strength cyclone, Sundarban alone can reduce the thrust force by more than 80%.

d. Artificial coastal afforestation is also effective to reduce the magnitude of thrust force. It is found that 1km afforested coastal belt can reduce the magnitude of thrust force by 40% to more than 65% depending on the landfall location of a cyclone. Increasing the width of afforestation will further reduce the impact of thrust force.

e. Model results show that magnitude of thrust force due to ‗cyclone wind only' is much less than the magnitude of thrust force due to combined action of ‗cyclone wind & surge wave'. This proves the observational evidence that the maximum damage caused by a tropical cyclone is due to the storm surge.

6.2 Limitation of the study

Following limitations are identified for the DFM:

1. The wind speed and surge depth is computed by a numerical model (Delft 3D). The DFM in its present form is not able to compute the surge depth independently.

2. The model is unable to compute the thrust forces when surge depth equals exactly to zero.

3. Because of the imposed initial and boundary conditions, it is not appropriate to apply the model in the ocean.

6.3 Recommended Future Study

Considering the above limitations, recommended future studies are:

1. DFM can be made independent by analytically solving the mass and momentum equations to compute the surge depth.

2. The zero-surge-depth problem needs to be solved mathematically.

3. Present version of DFM can be made a coupled module to the present version of Delft 3D. As Delft3D is open source, this coupling will make DFM to be used globally as part of Delft 3D.

RFERENCES

Abdou, M.A and Soliman, A.A., ―New Application of Variational Iteration Method‖.
2005.Nonlinear Phenomena,211, 1-8.

Abiodun, B.J., Salami, A.T., Matthew, O.J., Odedokun, S. (2013) Potential impacts of
afforestation on climate change and extreme events in Nigeria, Clim. Dyn 41: 277,
doi:10.1007/s00382-012-1523-9

Abrol, V., 1987. Application of a linear Surge Model for the Evaluation of Storm Surges
along the Coastal Waters of Kalpakkam, East Coast of India, Indian J. of Marine Sciences,
Vol. 16, pp.1-4.

Adomian, G., 1983. Stochastic System, Acad. Press, 1983.

Adomian, G., 1988. A Review of the Decomposition Method in Applied Mathematics, J.
Math. Anal. Applic., 135:501-544.

Adomian, G.A., 1988. Review of the decomposition method in applied mathematics, J. Math.
Anal. Appl. 135 (1988) 501—544.

Ali, A. 1980. Storm Surges in the Bay of Bengal and their numerical modeling. SARC Tech
Rep no. 120/80, Bangladesh Atomic Energy Commission, Dhaka

Ali, A. 1999. Climate change impacts and adaptation Assessment in Bangladesh. Climate
Research, CR special 6, Vol. 12, No.2/3, pp.109-116.

Ali, A., Chowdhury, J.U., 1997. Tropical cyclone risk assessment with special reference to
Bangladesh. MAUSAM (formerly Indian J Meteorol Hydrol Geophys) 48:305-322

Ali, A.1996. Vulnerability of Bangladesh to climate change and sea level rise through
tropical cyclones and storm surges. Water, Air and Soil Pollution 92:171-179.

Australian Aid, World Bank.―SAMOA Post-disaster Needs Assessment: Cyclone Evan
2012‖. 2013. Government of Samoa.

Bender, M.A., Ginis, I., Tuleya, G.R., Thomas, B., and Marchok, T. 2007. The operational
GFDL Coupled Huricane-Ocean Prediction System and a Summery of its performance,
3966, Mon. Wea. Rev., 135, 3965-3989, 2007.

Bengtsson, L., K. I. Hodges, and E. Roeckner, 2006. ―Storm tracks and climate change.
Journal of Climate 19: 3518-43‖.

Bessona, O., Kaneb, S. and Syc, M.,"On a 1D-Shallow Water Model: Existence of solution
and numerical simulations". 2007. International Conference in Honor of Claude Lobry.

Bulatov, O. V. ―Analytical and Numerical Riemann Solutions of the Saint Venant Equations
for Forward and BackwardFacing Step Flows.‖ Faculty of Physics, Moscow State
University, Moscow, 119992 Russia, 2013, ISSN 09655425, Computational Mathematics
and Mathematical Physics.

Burston, J.M., Nose, T. and Tomlinson, R. 2013. Real time numerical simulation of storm
surge inundation using high-performance computing for disaster management,
Queensland. MODSIM, December 2013, Adelaide.

References

Charnock, H., 1955. Wind stress on a water surface, Quart. J. Roy. Meteorol. Soc., 81, 639-640.

Charnock, H., 1955. Wind stress on a water surface, Quart. J. Roy. Meteorol. Soc., 81, 639-640, 1955.

Chezy, A. 1776. Formule pour trouver la vitesse de l'eau conduit dan une rigole donnée. Dossier 847 (MS 1915) of the manuscript collection of the École Nationaldes Ponts et Chaussées, Paris. Reproduced in: Mouret, G. (1921). Antoine Chézy: histoire d'une formule d'hydraulique. Annales des Ponts et Chaussées 61, 165-269.

Choudhury, S.A. 2014. Country Report of Bangladesh on Effective Tropical Cyclone Warning in Bangladesh, JMA/WMO Workshop on Effective Tropical Cyclone Warning in Southeast Asia Tokyo, Japan 11-14 March 2014.

Chow, V.T., Open Channel Hydraulics. McGrawHill Publishing Company, New York, 1959.

Chowdhury, A. M. 1981. Cyclone in Bangladesh. A Report, Bangladesh Space Research and Remote Sensing' Organization. Dhaka

Chowdhury, J.U. (2001), Hydro-geological Environment of the Ganges Delta and Issues of Water Resources Management, Keynote paper, Seminar at IEB HQ, Dhaka, 30th August 2001, Civil Engineering Division, The Institution of Engineers, Bangladesh

Chowdhury, J.U. 2007. Issues in Coastal Zone Management in Bangladesh. Institute of Water and Flood Management (IWFM). Bangladesh University of Engineering and Technology (BUET), February 6, 2008.

Chowdhury, J.U., Karim, M.F., 1996. A risk-based zoning of storm surge prone area of the Gnages Tidal Plain. Journal of Civil engineering, Institution of Engineering, Bangladesh 24(2), 221-233.

Chowdhury, J.U., Watkins, D.W., Rahman, M.R. and Karim, M.F. (1998), _Models for cyclone shelter planning in Bangladesh', Water International, vol. 23, No. 3, pp. 155-163, Journal of the IWRA, Carbondale, Illinois, USA

Das, P.K. 1972. A prediction model for storm surges in the Bay of Bengal. Nature, 239, 211-213.

Das, P.K., Sinha, P.C. and Balasubrahmanyam, V. 1974. Storm surges in the Bay of Bengal. Quart. J.R. Met. Soc. 100:437-449

Dasgupta, S. Muray S. Laplante B. and Wheeler, D. 2011. Exposure of Developing Countries to sea level rise and Storm Surges. Forthcoming in Climate Change.

Dasgupta, S., Huq, M. Khan, Z.H., Murshed, M., Ahmed, Z., Mukherjee, N., Khan, M.F. and Pandey, K. 2010. Vulnerability of Bangladesh to Cyclones in a Changing Climate: Potential Damages and Adaptation Cost. The World Bank Development Research Group Environment and Energy Team April 2010

Dasgupta, S.,*Laplante, B.** Murray, S.* Wheeler,D.***,2009. Climate Change and the Future Impacts of Storm-Surge Disasters in Developing Countries. Policy research working paper, World Bank.

Dasgupta, S.,Laplante, B., Murray, S. and Wheeler,D.,2009. ―Sea-Level Rise and Storm Surges: A Comparative Analysis of Impacts in Developing Countries". Policy research working paper, World Bank.

De Scally, F.A., 2008. Historoical Tropical cyclone activity and impacts in the cook islands. Pacific Science, 62, 443-459.

References

Debsharma, S.K., 2007. Numerical Simulations of Storm Surges in the Bay of Bengal, First JCOMM Scientific and Technical Symposium on Storm Surges, Seoul, Republic of Korea, 02-06 October, 2007.

Debsharma, S.K., 2009. Simulations of Storm Surges in the Bay of Bengal. Marine Geodesy Journal, 32(2):178-198.

Debsharma, S.K., Rahman, M.M., Nessa, F.F., 2014. Simulation of Cyclone ‗Aila-2009' by using WRF-ARW Model and Numerical Storm Surge Model. Monitoring and Prediction of Tropical Cyclones in the Indian Ocean and Climate Change, 2014, pp.263-273

Drews, C.W., 2013. Using wind setdown and storm surge on Lake Fire to calibrate the air sea drag coefficient. PLoS One, 8,DOI:101371/Journal.pone.0072510

Dube, S.K., Chittibabu, P., Sinha, T.S., Rao, A.D. and Murty, T.S.,2004. Numerical modeling of storm surge in the head Bay of Bengal using location specific model. Natural Hazard, 31(2), 437-453.

Dube, S.K., Rao, A.D., Sinha, T.S., Murty, T.S. and Bahualyan, N., 1997. Storm surges in the Bay of Bengal and Arabian Sea: The problem and its prediction. Mausam 48(2):283-304.

Dube, S.K., Sinha, P.C and Roy, G.D., 1985. The numerical simulation of storm surges along the Bangladesh coast, Dynamics of Atmosphere and Oceans, 9,121-133.

Dube, S.K., Sinha, P.C. and Roy, G.D., 1985.The numerical simulation of storm surges along the Bangladesh coast, Dynamic of Atmosphere and Oceans, 9, 121-133.

Dube,S.K. and Gaur, V.K., 1995. Real time storm surge prediction system for the Bay of Bengal. Current Science 68, 103 113.

Emanuel, K., 2005. Increasing destructiveness of tropical cyclones over the past 30 years. Nature: 436, 686-688.

Emanuel, K., R. Sundararajan, J. Williams. 2008. Hurricanes and Global warming: Results from Downscaling IPCC AR4 Simulations. Available at ftp://texmex.mit.edu/pub/emanuel/PAPERS/Emanuel_etal_2008.pdf

Finlayson, B.A. The Method of Weighted Residuals and Variational Principles, Academic Press, New York, 1972.

Flather, R.A. 1994. A storm surge prediction model for the northern Bay of Bengal with application to the cyclone disaster in April 1991. Jr Phys. Oceanography 24: 172-190.

GoB (2008). Cyclone Sidr in Bangladesh: Damage, Loss and Needs Assessment for Disaster Recovery and Reconstruction. MoFDM, Dhaka, Bangladesh.

GoB, 2008. Cyclone SIDR in Bangladesh: Damage, Loss and Needs Assessment for Disaster Recovery and Reconstruction. MoFDM, Dhaka, Bangladesh.

Gray, W.M., 1968. Global view of the origin of tropical disturbance and storms, Mon. Wea. Rev., 96:669-700.

Gray, W.M., 1975. Global view of tropical cyclone genesis. Bulletin of the American Meteorological Society, 56, 322.

Gray, W.M., 1998: The formation of tropical cyclones. Meteorology and Atmospheric Physicss, 67, 37-69.

Hagedorn,P., 1981. Non-linear Oscillations (translated by Wolfram Stadler), Clarendon Press, Oxford.

References

Haque, C.E., 1997. Atmospheric Hazards Preparedness in Bangladesh: A Study of Warning, Adjustments and Recovery from the April 1991 Cyclone, Natural Hazards, vol. 16, pp.181-202.

Harris, D.L., 1963. Characteristics of the Huricane Storm Surge. Technical Paper No.48, U.S. Weather Bureau, Washington, D.C.

He,J.H. ─Variational Iteration Method-Some recent results and new interpretations". Journal of Computational and Applied Mathematics. 207,3-17, 2007.

He,J.H. A new approach to non-linear partial differential equations, Commun. Non-linear Sci. Numer. Simulation 2 (4) (1997) 230—235.

He, J.H. ─Variational Iteration Method- a kind of non-linear analytical technique: some examples". International journal of non-linear Mechanics. 34,699-708. 1999.

He, J.H., 1997. Variational iteration method for delay differential equations, Commun. Non-linear Sci. Numer. Simulation 2 (4) (1997) 235—236.

He, J.H., 1998. Variational iteration approach to 2-spring system, Mech. Sci. Technol. 17(2) (1998) 221—223 (in Chinese).

He, J.H., 1998. Variational iteration method for non-linearity and its applications, Mechanics and Practice 20 (1) (1998) 30—32 (in Chinese).

He, J.H., 1999. Non-linear Oscillation with Fractional Derivative and its Approximation, Int. Conf. on Vibration Engineering 98, Dalian, China, 1988. J.-H. He / International Journal of Non-Linear Mechanics 34 (1999) 699–708 707

Henry, R.F., Duncalf, D.S., Walters, R.A., Osborne, M.J. and Muryt, T.S. 1997. A Study of tides and storm surges in offshore waters of the Meghna estuary using a finite element model. Mausum 48(4):5 19-530.

Higaki, M., Hayashibara, H. and Nozaki, F. 2011. Outline of the Storm Surge Prediction Model at the Japan Meteorological Agency, Office of Marine Prediction, Japan Meteorology

Holland, G.J., 1980. An analytic model of the wind and pressure profiles in hurricanes. Mon. Wea. Rev., 108,1212-1218.

Holland, G.J., 1997. The maximum potential intensity of tropical cyclones. Journal of the atmospheric Science, 54, 2519-2541.

Hoque, M. Mozzammel. ─Strategies and Measures to Reduce Cyclone Damage." In Cyclone Disaster Management and Regional/Rural Development Planning: UNCRD-CIRDAP Seminar, Phase III, 27-29 January, 1992, Chittagong, Bangladesh, 25-45. Nagoya, Japan: UNCRD, 1992.

Hoque, M.M. 1992. Strategies and Measures to Reduce Cyclone Damage. In Cyclone Disaster Management and Regional/ Rural Development Planning: UNCARD-CIRDAP Seminar, Phase III, 27-29 January, 1992, Chittagong, Bangladesh, 25-45, Nagoya, Japan:UNCARD.

Hoque, M.M., 1991. Field study and investigation on the damage caused by cyclones in Bangladesh :a report on the April 1991 cyclone; Cyclone damage in Bangladesh, report on field study and investigations on the damage caused by the cyclone in Bangladesh in 29-30 April 1991, United Nations Centre for Regional Development , Nagoya, Japan, 1991, pp.75.

References

IMD, 1979. Tracks on storms and depressions in the Bay of Bengal and the Arabian Sea 1877-1970. India Meteorological Department (IMD), New Delhi.

Inokuti, M., 1978. General use of the Lagrange multiplier in non-linear mathematical physics, in: S. Nemat-Nasser (Ed.), Variational Method in the Mechanics of Solids, Pergamon Press, Oxford, pp. 156—162.

International Workshop on Tropical Cyclone(IWTC). 2006. Statement on tropical cyclones and climate change. November, 2006, 13 pp. http://www.gfdl.noaa.gov/global-warming-and-hurricanes.

Islam, A.K., Haque, M.S. and Bala, S.K., 2010. Hydrologic Characteristics of Floods in the Ganges-Brahmaputra-Meghna (GBM) delta, Natural Hazards, 54(3): 797-811. DOI: 10.1007/s11069-010-9504.

Islam, M.S., Haque, M., 2004. The mangrove-based coastal and nearshore fisheries of Bangladesh: ecology, exploitation and management, Reviews in Fish Biology and Fisheries 14, pp.153-180.

Islam, R.M. & Ahmad, M. (2004), Living in the coast PROBLEMS, OPPORTUNITIES AND CHALLENGES, ICZMP project, WARPO, Dhaka. Islam, M.R., Ahmad, M., Huq, H. & Osman, M.S. (2006), State of the Coast 2006, ICZMP project, WARPO, Dhaka.

IWM and BISR, 2009. Use Existing Data on available Digital Elevation Models to prepare Useable Tsunami and Storm Surge Inundation Risk Maps for the Entire Coastal Region, Final Report, Volume II, DEM, Landuse and Geomorphology Maps, April 2009.

IWM, 2005. Impact assessment of climate change on the coastal zone of Bangladesh. Final Report, Institute of Water Modeling, Dhaka, Bangladesh, 37p.

J.H. He, J.H., 1997. Semi-inverse method of establishing generalized principles for fluid mechanics with emphasis on turbomachinery aerodynamics, Int. J. Turbo Jet-Engines 14 (1) (1997) 23—28.

Jacobson, L., 2013. Introduction to Artificial Neural Networks. The Project Spot; 5 December 2013. http://www.theprojectspot.com/tutorial-post/introduction-to-artificial-neural-networks-part-1/7.

Jarrell, J.D., Lewis, J.K. and Whitaker, R.E., 1982, Bay of Bengal- A system to evaluate storm surge threat, Final Report, Contact A.I.D./S.O.D/P.D.C-C0294, Science applications Inc., Moneterey, Californioa,66.

Johns, B. and Ali.A.,1980. The numerical modeling of storm surges in the Bay of Bengal, Quarterly Journal of the Royal Meteorological Society, 106, 1-18.

Karim, M.F. and Mimura, N., 2008. Impacts of climate and sea-level rise on cyclonic storm surge floods in Bangladesh, Global Environmental Change 18 (2008) 490-500.

Khalil, G. 1992. Cyclones and Storm Surges in Bangladesh: Some Mitigative Measures. Natural Hazards. Vol. 6, pp 11-24

Khan, S.R., 1995. Geomorphic Characterization of cyclone hazards along the coast of Bangladesh, ITC-MSc study.

Kim, G. and Barros, A. 2001. Quantitative Flood forecasting Using Multisensor Data and Neural Networks. Journal of Hydrology, 246, 45-62.

Kim, O.K., Yamshita, T. and Choi, B., 2008. H Coupled process-based cyclone surge simulation for the Bay of Bengal, Ocean Model, 25,132-143.

References

Kohno, M. and Higaki, M., 2006. The Development of a Storm Surge Model including the Effect of Wave set up for Operational Forecasting Meteorology and Geophysics, 57, 11-19, doi:10.2467/mripapers.57.11,2006.

Kubatko, E.J., Development, Implementation and Verification of hp- Discontinuous Galerkin Models for shallow Water Hydrodynamics and Transport PhD. Dissertation, 2005.

Kurian, N.P., Nirupoma, M.B. and Thomas, K.V., 2009: Coastal Flooding due to synoptic scale, meso-scale and remote forcings, Natural Hazards, 48, pp.259-273.

Large, W.G. and Pond, S., 1981. Open Ocean Momentum Flux Measurements in Moderate to Strong Winds, J. Phys. Oceanogr., 11, pp.324-336.

Lewis, M., Bates, P., Horseburgh, K.,Neal, J., and Schumann, G., 2012. A storm surge inundation model of the Northern Bay of Bengal using publically available data. Quartely Journal of the Royal Meteorological Society, 139(671), pp.358-369. Doi:10.1002/qj.2040.

Liao, S.J., 1997. Homotopy Analysis Method - A Kind of Nonlinear Analytical Technique not Depending on Small Parameters, Shanghai J. Mech., 18(3):196-200.

McBride, J.L., 1995. Tropical Cyclone Formation. Global perspectives on tropical cyclones, WMO/TD-No.693,289p.

Mooley, D.A. and Mohile, C.M., 1983. A study of cyclonic storms incident in the different sections on the coast around Bay of Bengal. Mausam. 34:139-152.

Moramarco, T.,Fan, F.,and Bras, R.L. Fellow, ASCE,. ―Analytical Solution for Channel Routing with Uniform Lateral Flow". 1999.Journal of Hydraulic Engineering.

MoWR.1999. Integrated Coastal Zone Management: Concepts and issues: A Government of Bangladesh Policy Note. Ministry of Water Resources, Dhaka, Bangladesh.

Mungkasi, S. and Wiryanto, L.H.,―On the relevance of a variational iteration method for solving Shallow water equations". Proceedings of the 7th SEAMS UGM International Conference on Mathematics and its Applications 2015.

Murata, S., Imamura, F., Katoh, K., Kawata, Y., Takahashi, S. and Takayama, T. 2011. TSUNAMI to survive from Tsnuami. Advanced Series on Ocean Engineering, Volume 32.

Murty, T.S. and El-Sabh, M.I., 1992. Mitigating the effects of storm surges generated by tropical cyclones: A proposal, Natural Hazards 6(3), pp.251-273.

Murty, T.S., Flather, R.A., Henry, R.F., 1986. The Storm Surge Problem in the Bay of Bengal, Progress in Oceanography, vol. 16, pp.195-233.

Napiorkowski, J.J., Dooge, J.C.I. ―Analytical solution of Channel flow model with downstream control". 2010. Hydrological Science Journal.

Nayfeh, A.H., 1985. Problems in Perturbation, Wiley, New York.

Needham, H., and Keim, B.D., 2011. Storm Surge: Physical Processes and an impact Scale. Recent Hurricane Research-Climate, Dynamics and Societal impacts, (eds) Anhtony Lupo, ISBN 978-953-307-238-8.

Neumann, C.J., 1993. Global Overview, Chapter 1, Global guide to tropical cyclone forecasting. WMO, Geneva.

Nicholls, R.J., Hanson, S., Herweijer, N. Patmore, S., Hallegatte, J., Corfee-Morlot, J., Chateau, R. and vulnerability to Climate Extremes. OECD Environment Directorate, Environment Working Papers No. 1.

References

Nihal, F.,Sakib, M.,Elahi, W.E., Haque, A. Rahman, M. and Rimi, R. A. "Sidr-Like Cyclones in Bangladesh Coast". Paper Proceedings of Environment Technology & Energy 2015(ISBN 978-955-4543-29-4)

NOAA, 1972. USA Coastal Zone Management Act (CZMA). Section 304, CZMA. http://coast.noaa.gov/czm/act/sections/#304.

Outline of the Storm Surge Prediction Model at the Japan Meteorological Agency, Masakazu Higaki, Hironori Hayashibara, Futoshi Nozaki, Office of Marine Prediction, Japan Meteorological Agency

Pattanyak, S., Mohanty, U.C., and Gopalakrishnan, S.G., 2014. Improvement in Track and Intensity Prediction of Indian Seas Tropical Cyclones with Vortex Assimilation. Monitoring and Prediction of Tropical Cyclonesin the Indian Ocean and Climate Change. pp.219-229. Springer.

Powell, M.D., Vickery, P.J. and Reinhold, T.A., 2003. Reduced drag coefficient for high wind speeds in tropical cyclones. Nature, vol. 422, March 20.pp.279-283.

Qayyun, M.F., 1983. Prediction of storm surges for Bangladesh coasts by empirical method: Results and discurchssions. Presented at the WMO-ESCAP Panel on Tropical cyclones, pp.22-29. March, Dhaka

R.E. Mickens, An Introduction to Non-linear Oscillations, Cambridge University Press, Cambridge, 1981.

Rahman, A.M., Rahman, A.M. (2013). Effectiveness of Coastal Bio-Shield for Reduction of the Energy of Storm Surges and Cyclones, Procedia Engineering Volume 56, 2013, Pages 676-685, doi:10.1016/j.proeng.2013.03.177

Raisinghania, M.D.,‖Fluid Dynamics", 2003, chapter-12, p-928-930. India.

Rao, Y.R.P., Chittibabu, P., Dube, S.K., Rao A.D. and Sinha, P.C., 1997. Storm Surge prediction and frequency analysis for Andhara coast of India. Mausam 48, pp.555-566.

Reid, R.O. and Bodine B.R., 1968. Numerical Model for storm surges in Galveston Bay. J. Waterway Harbour Div., 94 (WWI), pp.33-57.

Reid, R.O., 1957. Associate Professor of Oceanography A&.\I College of Texas "Modification of the quadratic bottom shear stress law for turbulent channel flow in the presence of surface wind stress".

Sakib, M., Nihal, F., Akter, R., Maruf, M., Akter, M., Haque, A., Rahman, M. ‖Afforestation as a Buffer against Storm Surge Flooding along the Bangladesh Coast". 12thInternational Conference on Hydroscience & Engineering 2016 (accepted), 2016.

Sakib, M., Nihal, F., Haque, A., Rahman, M., and Ali, M., (2015). Sundarban as a Buffer against Storm Surge Flooding, World Journal of Engineering & Technology, VOL. 3, PP. 59-64.

Sakib, M., Nihal, F., Haque, A., Rahman, M. and Ali, M. "Sundarban as a Buffer against Storm Surge Flooding", 2015. World Journal of Engineering and Technology, 2015, 3, 59-64.

Sielecki, A. and Wurtele, M.G., 1970. The numerical integration of the nonlinear shallow-water equations with sloping boundaries. J. Comput. Physics, 6, pp.219-236.

Sinha, P.C., Dube, S.K. and Roy, G.D., 1985. Influence of river on the storm surges in the Bay of Bengal, Proc. International workshop on operational application of mathematical models in developing countries, 26 February-1 May, New Delhi, India.

References

Smith, S.D. and Banke, E.G., 1975. Variation of the sea surface drag coefficient with wind speed, Quart, J. Roy. Meteorol. Soc., 101, pp.665-673.

Trucano, T.G., L.P. Swiler,L.P.. Igusa,T., Oberkampf, W.L. Pilch, M. 2006. Calibration, validation, and sensitivity analysis: What's what. Reliability Engineering and System Safety 91 (2006) 1331–1357

Vreukdenhil, C.D. ‖Numerical Method for Shallow water equations". Boston: kluwer Academic publishers, 1994.

Webster, P.J., Holland, G.J., Curry, J.A., and Chang, H.R. (2005). Changes in tropical cyclone number, duration, and intensity in awarming environment. Science, 309, 1844–1846.

World Bank (2010). Ecomics of Adaptation to Climate Change Bangladesh, World Bank, Ministry of Forieng Affairs Government of Netherlands, DFID United Kingdom, Swiss Agency for Development and Cooperation SDC. © 2010 The World Bank Group.

Y. Cherruault, Convergence of Adomian's Method, Kybernets 18 (2) (1989) 31—38.

Yen, Ben Chie. 2004. Channel Flow Resistance: Centennials of Manning's formula. USA: Water Resources Publication, LLC, Highlands Ranch Colorado, 80163- 0026, 158.

Yuvaraj, E., Dharanirajan, K., Saravanan and Narshimulu, G., ‖Post-disaster assessment of impact of cyclone Lehar in South Andaman Island". 2015.Department of Disaster Management, Pondicherry University, Port Blair 744 112, India

Zhai, X., Johnson, H.L.,Marshall, D.P. and Wunsch, C.‖On the Wind Power Input to the Ocean General Circulation".2012. American Meteorological Society, United Kingdom.

Zhizua, Z., Wang, Y., Yihong, D., Lianshou, C., Zhiqiu, G., 2010. On Sea Surface Roughness Parameterization and Its effect on tropical Cyclone Structure an dIntensity. Advances in Atmospheric Sciences, vol. 27, no.1-4, 2004. pp.98-117.